


Review

# Recent Advances in Smart Fabric-Type Wearable Electronics toward Comfortable Wearing

Hong Xiang<sup>1</sup>, Yongfu Li<sup>1</sup>, Qinglong Liao<sup>1</sup>, Lei Xia<sup>1</sup>, Xiaodong Wu<sup>1</sup>, Huang Zhou<sup>2</sup>, Chunmei Li<sup>3,\*</sup> and Xing Fan<sup>4,\*</sup> 

<sup>1</sup> State Grid Chongqing Electric Power Research Institute, Chongqing 401221, China; xhhyde123@163.com (H.X.); lyf\_ee@163.com (Y.L.); qinglongliao@163.com (Q.L.); xialei023@163.com (L.X.); parker9216@126.com (X.W.)

<sup>2</sup> School of Pharmacy and Institute of Pharmacy, North Sichuan Medical College, Nanchong 637100, China; zhouhuangcbyxy@163.com

<sup>3</sup> College of Materials Science and Engineering, Chongqing University, Chongqing 400044, China

<sup>4</sup> College of Chemistry and Chemical Engineering, Chongqing University, Chongqing 400044, China

\* Correspondence: may840@cqu.edu.cn (C.L.); foxcqx@cqu.edu.cn (X.F.)

**Abstract:** With the improvement of the energy density and sensing accuracy of wearable devices, there is increasing interest in applying wearable electronics in daily life. However, traditional rigid plate-structured wearable devices cannot meet the human body's wearing habits and make users may feel uncomfortable after wearing them for a long time. Fabric-type wearable electronics can be conformably coated on human skin without discomfort from mismatches in mechanical properties between the human body and electronics. Although state-of-the-art textile-based wearable devices have shown unique advantages in the field of e-textiles, real-world scenarios often involve stretching, bending, and wetting. Further efforts should be made to achieve "comfortable wearing" due to the great challenge of achieving both promising electrical properties and comfort in a single device. This review presents a comprehensive overview of the advances in smart fabric-based wearable electronics toward comfortable wearing, emphasizing their stretchability, hydrophobicity, air permeability, stability, and color-change abilities. Through addressing the challenges that persist in fabric-type wearable electronics, we are optimistic that these will be soon ubiquitous in our daily lives, offering exceptionally comfortable wearing experiences for health monitoring, sports performance tracking, and even fashion, paving the way for a more comfortable and technologically advanced future.

**Keywords:** wearable electronics; fabric-type; multiple functions; comfortable wearing



**Citation:** Xiang, H.; Li, Y.; Liao, Q.; Xia, L.; Wu, X.; Zhou, H.; Li, C.; Fan, X.

Recent Advances in Smart Fabric-Type Wearable Electronics toward Comfortable Wearing. *Energies*

2024, 17, 2627. <https://doi.org/10.3390/en17112627>

Academic Editor: Haizeng Li

Received: 29 April 2024

Revised: 24 May 2024

Accepted: 27 May 2024

Published: 29 May 2024



**Copyright:** © 2024 by the authors. Licensee MDPI, Basel, Switzerland. This article is an open access article distributed under the terms and conditions of the Creative Commons Attribution (CC BY) license (<https://creativecommons.org/licenses/by/4.0/>).

## 1. Introduction

Wearable electronics have been dramatically developed in recent years in fields including healthcare monitoring, sensing, wearable displays, and energy harvesting and storage [1–5]. However, due to limitations in current materials and technologies, these devices are typically constructed with rigid electronic components affixed to flexible substrates. The mechanical mismatch between rigid electronics and the human body makes people feel uncomfortable with long-term on-body applications [6].

Since wearable electronics are mostly in contact with the human body, textiles are considered to be a suitable platform for daily and long-term applications [7]. Textiles are made up of fibers, which can provide excellent softness, extensive surface areas, and high porosity. These properties are of paramount importance for the advancement of wearable device technology, as they facilitate the seamless integration of electronic materials into the porous textile structures without compromising the electronic functionality and the textiles' potential softness [8–12]. In the context of the development of fabric-type wearable electronics toward comfortable wearing in the future, there is a high demand for devices with stretchability, hydrophobicity, air permeability, color-change ability, and durability [13–15].

In terms of stretchability, researchers have explored the integration of conductive materials with stretchable substrates or specialized structural electrode designs to ensure the stretchability of these wearable textiles in complicated working environments [16–18]. In addition to stretching, water intrusion frequently occurs in daily life scenarios, often resulting in degradation of performance for fabric-type wearable electronics. To address this issue, researchers have developed novel superhydrophobic surfaces for wearable devices. These developments have been proposed from two aspects: coating materials and preparation methods [19–22]. Furthermore, wearable electronics with excellent air permeability have the ability to allow gases, moisture, and liquids to pass through while still functioning when attached to the human body. This ensures a biocompatible interface between devices and human skin, which is beneficial for long-term and real-time monitoring of human health in a noninvasive and imperceptible manner [23–25]. Numerous studies have been conducted on the impact of textile material and structure on the air permeability of wearable electronics [26–29]. In addition, the durability of fabric-type wearable electronics needs to be examined under various deformations, including their mechanical stability, chemical stability, and further operational stability in complex environments, before being applied to practical applications [30].

Notably, there is a growing interest in the research into smart color-changeable textiles, due to their significant potential for application in non-emitting displays, sensing, military camouflage, optical recording, environmental monitoring, and camouflage [31–36]. Researchers have conducted extensive research and have found that color-changing materials are the most crucial factor influencing the color-change ability of textiles.

This review offers an overview of the progress achieved in the development of smart electronic textiles toward comfortable wearing. It mainly covers their stretchability, hydrophobicity, stability, air-permeability, and color-change ability, as well as discussing the existing challenges.

## 2. Stretchability of Smart Fabric-Type Wearable Electronics

Wearable electronics have attracted significant attention due to their unprecedented potential in sensing, healthcare, and data transmission. As we know, wearable electronics operate during the complex daily working environment, where they inevitably encounter issues such as stretching. The concept of stretchability refers to the ability to maintain conductive pathways under significant strains ( $\gg 1\%$ ) and restore their original properties after releasing the induced strain [37]. This capability is considered a key point of wearable electronics. Unfortunately, traditional wearable electronics based on monocrystalline silicon or metal oxide films have always exhibited high rigidity due to their inherent brittleness, which has significantly hindered their use in stretching working environments.

The advancements in stretchable wearable electronics have the potential to alleviate discomfort caused by mismatches in mechanical properties between the human body and wearable electronics. Recently, significant efforts have been dedicated to the development of stretchable wearable electronics, focusing on two key aspects: conductive materials and geometrically engineered structures.

### 2.1. Stretchable Electrode Based on Conductive Materials

Typically, conductive materials are commonly used as the building blocks for constructing conductive interconnects and electrodes for wearable electronic devices. In comparison to traditional conductive materials such as monocrystalline silicon, novel conductive materials demonstrate unique electrical properties that include enhanced conductivity and reduced resistance and capacitance. These properties make them ideal fundamental components in the development of stretchable wearable electronics. This subsection covers two types of novel conductive materials demonstrated for emerging stretchable wearable electronics, including organic conductive materials and inorganic conductive materials [38–58].

Firstly, regarding organic conductive materials, conducting polymers have been predominantly utilized in the development of stretchable conductors due to their flexible and

highly conductive characteristics. Examples include poly (3,4-ethylenedioxythiophene) polystyrene sulfonate (PEDOT: PSS) [38], poly (3-butylthiophene-2,5-diyl) (P3BT) [39], polyurethane (PU) [49,50], polyaniline (PANi) [51], and so on. Among them, PEDOT: PSS is widely utilized due to its high transmittance and excellent conductivity. In a recent study by Bao et al. [38], a highly stretchable all-polymer light-emitting diode (APLED) was developed through modifying PEDOT: PSS to enhance both stretchability and electrical conductivity, as depicted in Figure 1a. It was found that the fabricated stretchable APLED demonstrated the capability to withstand up to 100% strain while maintaining approximately 85% of its original brightness even after being stretched for 100 cycles to 40% strain. Meanwhile, PthTFB has been employed in the development of stretchable conductors. Ren et al. [39] fabricated a polymer based on PthTFB that exhibited exceptional stretchability and electrical conductivity during more than 1000 cycle durability tests (Figure 1b). In addition, Bao et al. [40] proposed a DPPT-TT-based stretchable film that benefited from the nanoconfinement of polymers. This led to an improvement in the stretchability of polymer semiconductors without affecting charge transport mobility. As a result, the fabricated semiconducting film can be stretched up to 100% strain without affecting mobility (Figure 1c). Another approach to enhancing the conductivity and stretchability of conducting polymers involves addressing the issue of disconnected nanoaggregates caused by poor miscibility of components. For example, Zhao et al. [41] developed an interconnected and densely arranged conductive polymer network using PANi-based precursor materials. This conductive polymer network demonstrated the ability to be easily stretched to 200% of its initial length without breaking (Figure 1d).

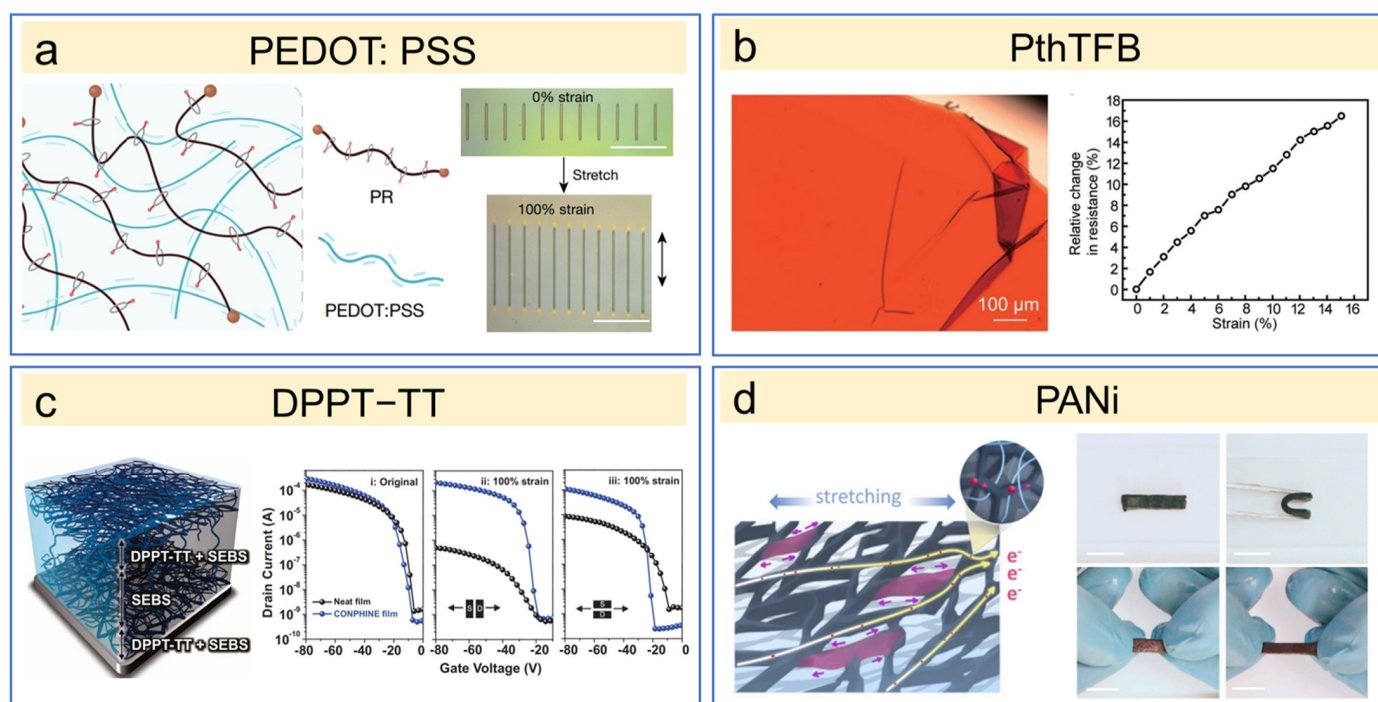


**Figure 1.** Conductivity of various types of organic conductive materials: (a) The structure of the PEDOT: PSS-based light-emitting film (reprinted with permission from Ref. [38]. Copyright 2022 Springer Nature); (b) Photograph of PthTFB and the relative change in resistance under strain (reprinted with permission from Ref. [39], copyright 2018 John Wiley & Sons, Inc.); (c) A 3D illustration of the morphology of the DPPT-TT-based film and its transfer curves under strain (reprinted with permission from Ref. [40], copyright 2017 The National Academy of Sciences of the USA). (d) The structure of the PANi-based device (reprinted with permission from Ref. [41], copyright 2020 Elsevier).

Secondly, regarding inorganic conductive materials, carbon-based and metal-based materials have been extensively researched (Figure 2a–f).

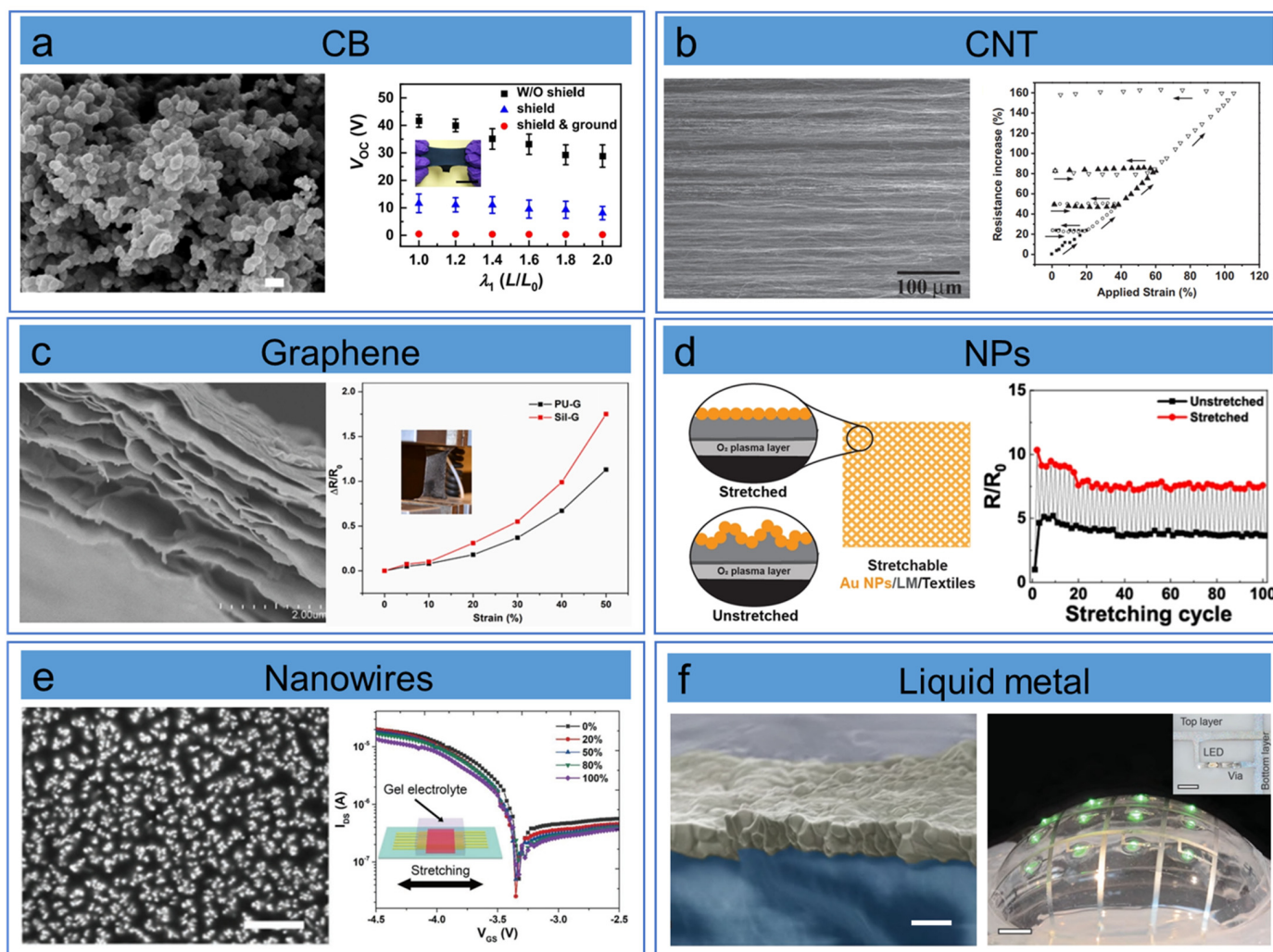


**Figure 2.** Conductivity of the inorganic conductive materials: (a) Operation mechanism of the CB-based device and the response was monitored at different angles (reprinted with permission from Ref. [42], copyright 2024 Springer Nature); (b) Top-view scanning electron microscope (SEM) image of a CNT ribbon and the resistance change of a typical CNT/PDMS film as a function of applied strain (reprinted with permission from Ref. [43], copyright 2012 John Wiley & Sons, Inc.); (c) SEM images of the freeze-dried graphene aerogel and resistance change of graphene aerogel-based films under stretching (reprinted with permission from Ref. [44], copyright 2020 Elsevier); (d) Schematic illustration depicting the fabrication steps of stretchable electronic textiles and their corresponding linear resistance with stretching cycles (reprinted with permission from Ref. [45], copyright 2023 American Chemical Society); (e) Top-view SEM image of a stretchable transistor based on AuNWs at different strain (reprinted with permission from Ref. [46], copyright 2018 John Wiley & Sons, Inc.); (f) Stretchable electrode based on biphasic gold-gallium thin films (reprinted with permission from Ref. [47], copyright 2016 John Wiley & Sons, Inc.).

On the one hand, carbon-based materials such as carbon black (CB) [52], CNTs [53], and graphene [54], have been investigated. CB is a paracrystalline form of carbon that serves as a fundamental component for the construction of conductive networks due to its exceptional thermal/electrical conductivity and commercially viable properties. Lai et al. [42] developed a stretchable multiplexing triboelectric e-skin utilizing elastic CB-doped Ecoflex as the shielding layer and electrode. Specifically, through the design of a conductive CB-based stretchable shielding layer, the triboelectric e-skin maintained its functionality even under 400% isotropic strains (Figure 2a). However, the conductivity of such an electrode is limited due to the low conductivity of the percolation network formed of CB

particles. In comparison to the electrical and mechanical properties of CB, CNTs possess high aspect ratios which make them more suitable materials for enhancing conductivity in stretchable electrodes. Xu et al. [43] fabricated a conductive electrode by employing multi-walled carbon nanotubes (MWCNTs) on a polydimethylsiloxane (PDMS) substrate. It was observed that the resistance remained constant within the strain range of 0–100% after multiple stretch–release cycles, which was attributed to the effective penetration of carbon nanotubes into the PDMS network (Figure 2b). Compared with CB and CNTs, graphene-based materials have become increasingly popular due to their superior electrical and mechanical properties. Chen et al. [44] prepared a graphene-based stretchable electrode through incorporation of polyurethane and interconnected graphene gels (Figure 2c). The resulting graphene network demonstrated a resistance deviation of less than 5% even after 500 bending cycles.

On the other hand, metal-based materials such as nanoparticles (NPs) [55], nanosheets [56], flakes [57], nanowires (NWs) [58], and liquid metal (LM) have been extensively utilized in the fabrication of wearable electronics. For instance, Lee et al. [45] introduced Au NP layers on LM-based electronics, as shown in Figure 2d. Specifically, the flexible textile displayed stable resistance after 100 stretching cycles. Additionally, metallic NWs such as Au, Ag, and Cu have recently garnered significant attention due to their high aspect ratio and high intrinsic conductivity. For example, through integrating the advantages of both top-down patterning and bottom-up synthesis, the stretchable electrode based on AuNWs exhibited a conductivity of  $152 \text{ S cm}^{-1}$  at 170% strain [46]. Furthermore, liquid metals can undergo significant deformations while maintaining electrical continuity, making them promising materials for the development of stretchable devices. As depicted in Figure 2f, a stretchable green surface-mounted light-emitting diode matrix was interconnected and powered through the use of a liquid metal-based conductor [47].

In general, despite the reasonable conductivity exhibited by the aforementioned stretchable conductive materials, a significant challenge arises in their application in devices, specifically pertaining to the decrease in conductivity under applied strain. This reduction occurs under conditions of elevated strain, where the deformation of the elastic matrix leads to a decrease in interfacial contact between the nanoparticles, thereby affecting their overall conductivity.

## 2.2. Stretchable Electrode-Based Structural Electrode Designs

As mentioned previously, the conductivity of conductive materials decreases under conditions of increased strain, due to the reduction of the contact area among nanomaterials or structural deformation of the molecular chain. Alternatively, a prevailing method for achieving stretchability arises from specific geometrical configurations, encompassing kirigami structures, buckling structures, island–bridge structures, and serpentine patterns, enabling materials to maintain their electrical properties while undergoing significant deformation [59–63].

Firstly, a kirigami structure inspired by paper cutting techniques can equip the electrodes with high stretchability through employing thin sheets of elastic material to adapt their formation. During the initial elastic deformation, the mechanical stress is mainly concentrated at the connection nodes. Under extreme external conditions, the stress distribution undergoes a significant transformation, redirecting the stress toward bending and torsional deformations. This redistribution effectively mitigates the mechanical strain imposed on the active device component, thereby enhancing its durability and stability. This mechanism ensures the reliable operation of the device even under challenging environmental conditions. For example, Lu et al. [59] developed a G-PMDS/RGO strain sensor exhibiting a substantial workable strain range, leveraging a kirigami structure. This innovative design conferred exceptional deformation capability to the strain sensor, enabling an ultra-large working range extending up to 350% (Figure 3a).

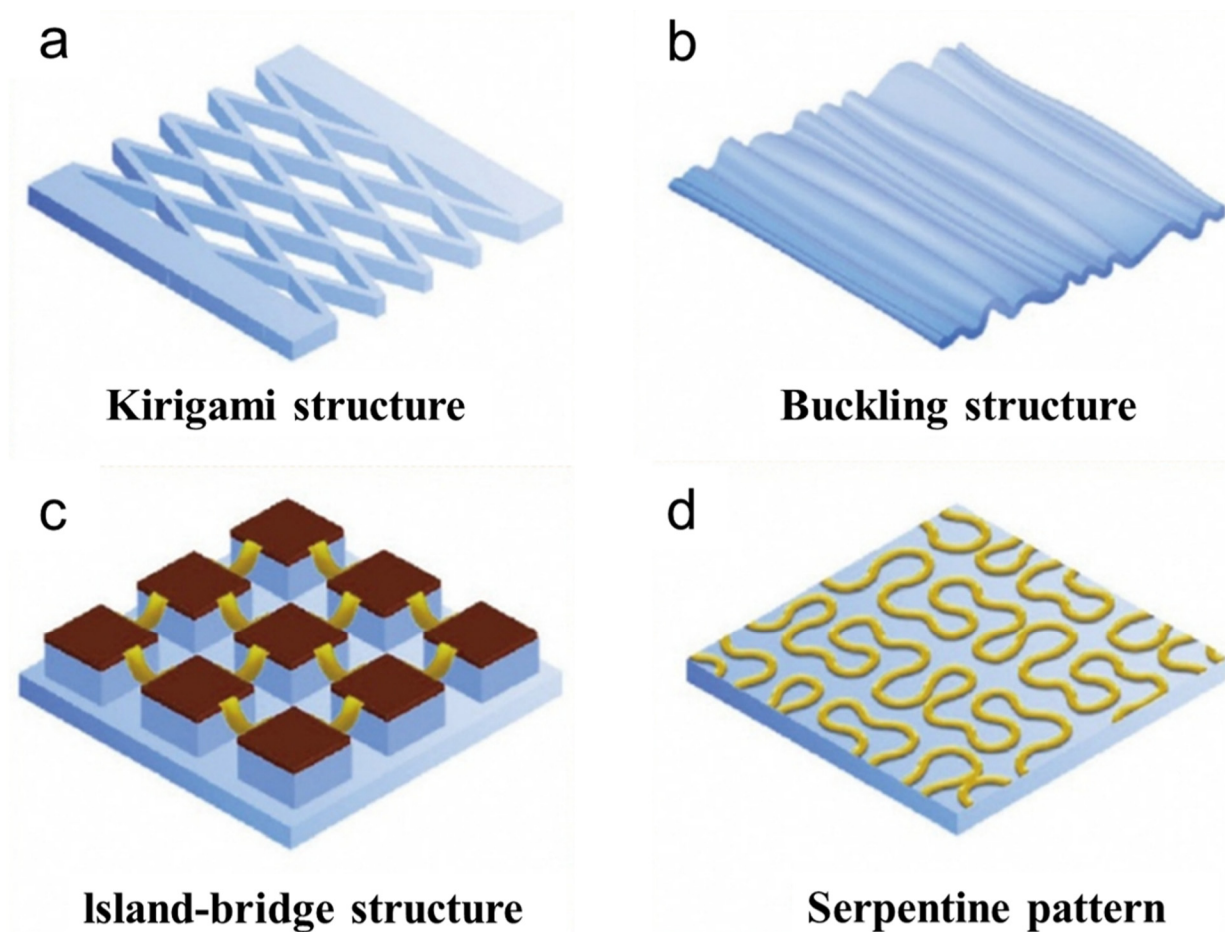


**Figure 3.** The diverse range of stretchable structural designs: (a) kirigami structure; (b) buckling structure; (c) island–bridge structure; (d) serpentine pattern (reprinted with permission from Ref. [63], copyright 2024 The Royal Society of Chemistry).

Secondly, the design of a buckling structure enables the device to undergo stretchable movements within the pre-stretched strains of the supporting elastomers. This refers to those stretchable devices that exhibit a controlled and reversible deformation mechanism, typically in the form of folds or wrinkles, when subjected to tensile forces. These structures are specifically designed to accommodate significant stretching without compromising their overall integrity or functionality. As illustrated in Figure 3b, a prestrain–release–buckling strategy was utilized to align CNT sheets (NTS) around stretched rubber fiber cores [60]. Leveraging the hierarchically buckled structure, the fibers exhibited a resistance change of less than 5% under a 1000% stretch.

Thirdly, the island–bridge structure involves the positioning of rigid and functional electronic devices on an array of islands made of a stretchable substrate, connected via stretchable conductors as signal output bridges. The microstructure conductor exhibits greater flexibility than the rigid device, allowing the deformation of the entire system to be primarily concentrated within the conductor. This ensures that the rigid device experiences less than 1% strain. For example, Lee et al. [61] designed stretchable electronics using an island–bridge structure. It was found that the regularly positioned bumps and valleys in a hexagonal-closed-packed structure contributed to increased stability for the layers and devices on the substrate under multidirectional stretching (Figure 3c).

Fourthly, in order to improve the stretchability of the device using an island–bridge design, a serpentine pattern of stretchable conductors has also been introduced. Choi et al. [62] demonstrated a serpentine pattern structure by inserting a giant twist into spandex-core fibers wrapped in a carbon nanotube sheath. The resulting supercoiled fibers exhibited a

highly ordered and compact structure along the fiber direction, capable of sustaining up to 1500% elastic deformation (Figure 3d).

Overall, while the stress distribution within the 3D serpentine pattern exhibits a more uniform characteristic compared with other structures, such as the 2D open-mesh configuration, 3D structures possess inherent complexities in their mechanical properties, thermal expansion coefficients, and manufacturing processes. These complexities pose significant challenges in terms of scalability and commercialization, potentially hindering the widespread application of these structures. Therefore, further research is necessary to address these complexities and develop efficient strategies for large-scale production and implementation of 3D coiled structures.

### 2.3. Assembling of Smart Fabric-Type Stretchable Devices

The attainment of stretchability in wearable electronic devices capable of enduring diverse mechanical deformations encountered during daily use serves as the fundamental prerequisite toward comfortable wearing. Recently, there has been a surge of interest in the development of stretchable fabric-based wearable devices that exhibit robust performance even under conditions of high tensile strain or significant deformation. This is primarily attributed to their diverse and multifunctional applications, encompassing areas such as stretchable supercapacitors, solar cell textiles, sensors, and triboelectric nanogenerators. These devices offer the potential to revolutionize the wearable-technology industry by providing flexible and conformable solutions that can adapt to the contours of the human body and withstand the rigors of daily use. As such, they have the potential to significantly enhance the performance and usability of wearable electronics, opening up new avenues for innovative applications in health monitoring, sports performance tracking, and personal entertainment systems [64–67].

Firstly, supercapacitors have garnered significant attention for their applications in wearable devices, owing to their noteworthy high-power density and remarkable cycle stability. Park et al. [68] made a noteworthy contribution in this field, developing a stretchable, high-performance supercapacitor specifically designed to power an integrated sensor within a textile system (Figure 4a). Notably, that study revealed that even after undergoing 5000 cycles of stretching and releasing, with strain gradually increasing from 10% to 50%, the supercapacitor retained approximately 80% of its initial capacitance. This remarkable performance underscores the potential of supercapacitors for powering wearable devices, even under conditions of significant mechanical deformation.

Secondly, stretchable solar cells that possess the capability to withstand substantial strain and exhibit superior cyclic mechanical resilience pose significance for application in wearable and skin-interfaced electronics. Son et al. [69] successfully demonstrated a stretchable solar cell that exhibited remarkable stretchability and stability, which had been fabricated by introducing conductive polymers and ionic liquids into an intricate network of wavy silver nanowires. Remarkably, it was found that the solar cells were able to retain 89% of their initial efficiency even under a tensile strain of 20% (Figure 4b). This advancement offers promising potential for use in wearable electronic devices, where the requirement for flexibility and durability is paramount. Furthermore, the development of a stretchable photo-rechargeable energy fabric was achieved through the integration of stretchable solar cells with stretchable batteries [70]. The application of strain was quantified through meticulously calculating the distances between fixed edges, comparing measurements taken prior to and subsequent to the stretching process. As depicted in Figure 4c, the unique structure of the energy fabric enabled it to maintain stable output characteristics, specifically an  $I_{sc}$  of 123  $\mu\text{A}$  and  $V_{oc}$  of 0.36 V, even under a strain of 100%. This demonstration underscores the fabric's resilience and efficacy in maintaining its functional properties despite significant deformation.

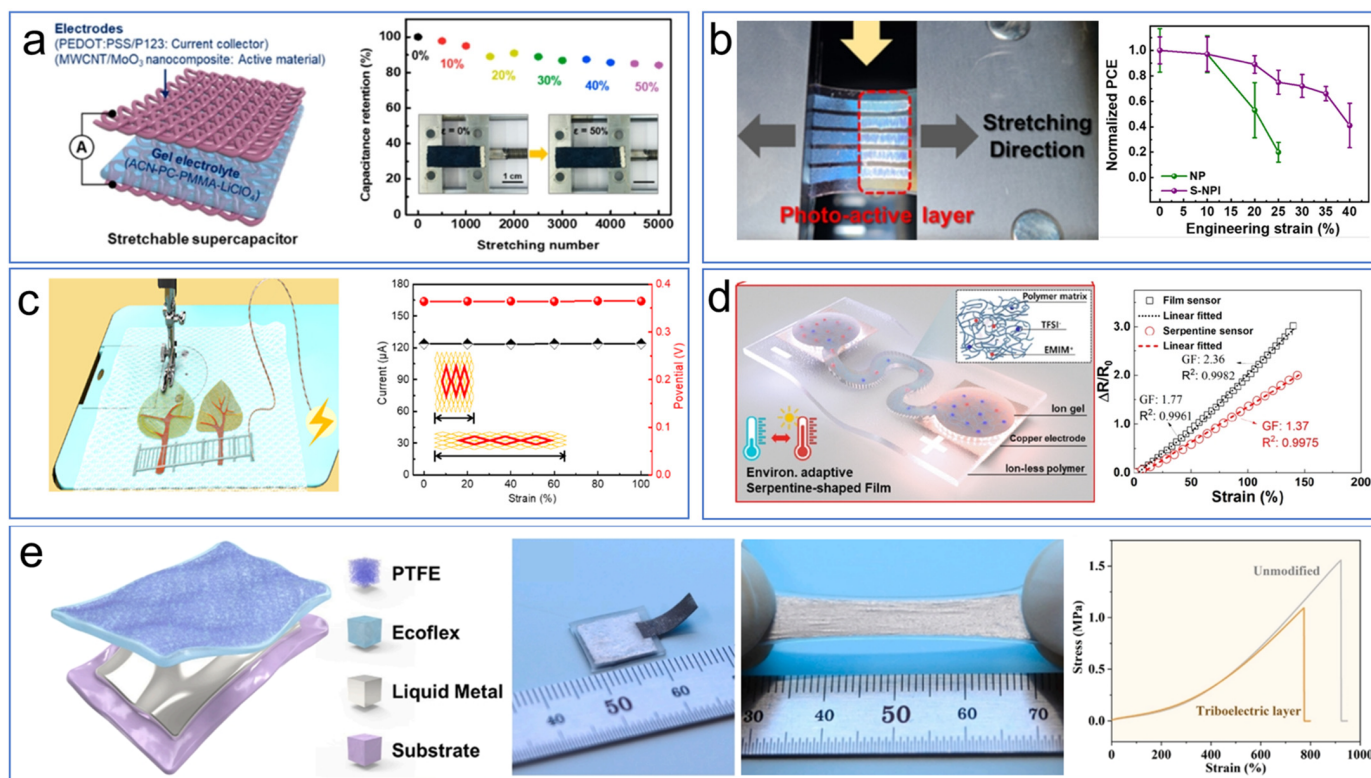


**Figure 4.** Stability testing of smart wearable electronic devices: (a) Stretching test of the supercapacitor consisting of MWCNT/MoO<sub>3</sub> nanocomposite electrodes (reprinted with permission from Ref. [68], copyright 2019 American Chemical Society); (b) Photographic images of the stretchable organic solar cells and in situ stretching test (reprinted with permission from Ref. [69], copyright 2023 American Chemical Society); (c) The stable performance of the energy fabric under different strain (reprinted with permission from Ref. [70], copyright 2020 American Chemical Society); (d) Comparison of the relatively resistive output between film sensor and serpentine sensor (reprinted with permission from Ref. [71], copyright 2024 American Chemical Society); (e) The performance of the stretchable triboelectric nanogenerator under different strain (reprinted with permission from Ref. [72], copyright 2023 Elsevier).

Thirdly, there has been extensive research and development in the field of stretchable sensors for applications such as human–machine interaction. Kim et al. [71] demonstrated a stretchable sensor with exceptional stress–strain linearity and remarkable durability (>100,000 cycles), through conformally laminating it onto body joints for human gesture recognition. The sensor demonstrated high accuracy and consistency even under stress exceeding 150%, and was based on a plane structure design, as illustrated in Figure 4d. That work provided valuable insights into the development of highly responsive and resilient stretchable sensors for various applications in human–machine interaction and wearable technology.

Fourthly, the development of stretchable triboelectric nanogenerators (TENGs) serves as an efficient strategy to tackle the energy constraints faced by smart wearable devices. Chen et al. [72] demonstrated a stretchable TENG textile capable of harvesting droplet energy across diverse scenarios (Figure 4e). It was found that the output decline of the TENG textile remained below 20% even under a stretch rate of 500%, highlighting its stretchability under demanding conditions.

As discussed above, stretchable wearable devices have been largely contingent on the advancement of stretchable electrodes possessing both high conductivity and exceptional stretchability, and the performance of the stretchable electrodes depends significantly on the properties of the conductive materials (e.g., conductive polymer, carbon nanomaterials,



metal nanostructure) and the electrode's structural design (e.g., open-mesh structure, buckling structure, island–bridge structure, or serpentine pattern). Regarding conductive materials, these have been incorporated into elastomeric substrates to fabricate stretchable conductive electrodes with desired conductivity. In terms of the electrode's structural design, it has been empirically demonstrated that the introduction of diverse structures can significantly enhance the overall stretchability of wearable devices. These advancements significantly broaden the potential applications for stretchable electrodes, offering new horizons in the realm of wearable electronics, thus advancing the field toward more innovative and practical solutions.

### 3. Hydrophobicity of Smart Fabric-Type Wearable Electronics

In addition to stretching, water intrusion is a common occurrence in daily life, posing significant challenges to the performance of wearable electronics. Therefore, it is important for researchers to develop strategies to protect wearable electronics from water damage and excessive moisture in order to ensure their long-term performance and usability. Conventional hydrophobic fabrics are fabricated through coating with hydrophobic agents, such as fluorine-containing finishing agents, which cause significant environmental pollution during the preparation process. Moreover, the leakage of electrolytes resulting from device damage also poses a potential risk of harm to human skin. Superhydrophobic surfaces have garnered considerable attention due to their distinctive water-repellent characteristics, stability, and environmental friendliness [73,74]. These properties render them highly promising for various applications that require effective resistance to water intrusion. As a result, many strategies to create superhydrophobic surfaces for the wearable devices have been put forward from the two aspects of coating materials and preparation methods, helping wearable electronics to effectively shed water and work stably even in humid environments.

#### 3.1. The History of Conventional Hydrophobic Fabrics

Figure 5 summarizes the development of traditional fabric hydrophobic treatments. Since the 1930s, there has been a significant focus on the development of hydrophobic textiles within the textile industry, which has served as a focal point for driving advancements in the field. Conventionally, hydrophobic fabrics have been fabricated through the application of hydrophobic agents, encompassing reactive aliphatic compounds, organosilicones, and fluorine-containing finishing agents. Utilizing aliphatic compounds as an illustrative example, reactive aliphatic compounds, characterized by long carbon chains terminated with reactive groups, are employed to modify textile surfaces, thereby achieving enduring water-repellent effects.

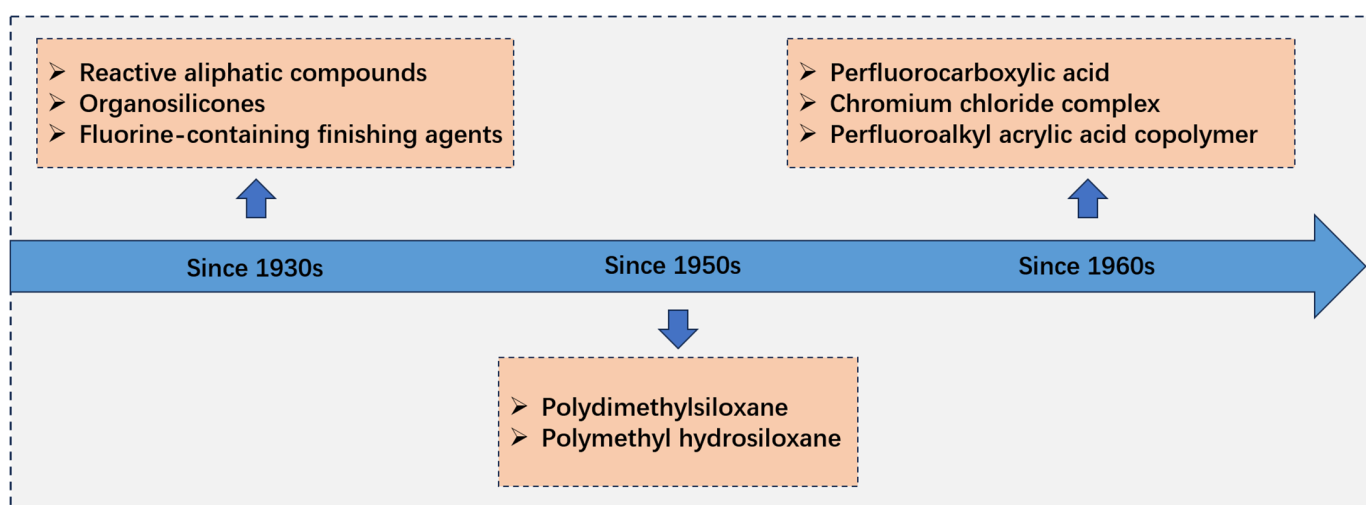


Figure 5. Development of traditional hydrophobic treatments for fabric.

Since the 1950s, polysiloxane has emerged as a significant organosilicon water-repellent agent in the textile industry. It is primarily used for treating polyester–cotton blended fabrics and vinegar-fiber fabrics destined for rainwear applications. Notably, zirconium or titanium compounds, known for their hydrolyzable properties, were often combined with polydimethylsiloxane (PDMS) and subsequently applied to fabric surfaces, yielding hydrophobic fabrics.

From the 1960s onward, following the entry of organosilicon water-repellent agents into the realm of textile chemical processing, the 3M Company (St. Paul, Minnesota) in the United States introduced several innovative products, including perfluorocarboxylic acid and chromium chloride complexes as well as perfluoroalkyl acrylic acid copolymers. These advancements not only conferred water repellency to textiles but also introduced a novel oil-repellent functionality. Toward the end of the 1980s, there was a significant development in hydrophobic textile technology with the introduction of super water-repellent textiles. This advancement expanded the potential applications of hydrophobic textile technology and made a notable impact on the market. In the 1990s, researchers introduced the concept of superhydrophobicity, which garnered widespread attention due to its remarkable properties of water repellency, scalability, and environmental friendliness. This innovation has since paved the way for the development of advanced hydrophobic materials, pushing the boundaries of textile technology and opening new avenues for diverse applications.

### 3.2. The Development of Hydrophobic Coatings

Superhydrophobic coating is essential for ensuring the stable operation of wearable devices in high humidity conditions. It can be achieved by applying various types of coating materials to the surface of the devices [75–79]. The classification of superhydrophobic coating materials can be divided into three primary categories: inorganic materials, organic materials, and inorganic–organic composite materials. In terms of coating methods, these encompass a range of techniques, including covalent layer-by-layer assembly, polymer roughening, sol–gel processing, chemical vapor deposition, and hydrothermal synthesis [80–82]. These methods offer a range of approaches for depositing coatings onto surfaces, each with its own unique set of advantages and applications.

Firstly, inorganic materials primarily encompass silicon-based materials, carbon-based materials, and metal oxides. Silicon-based materials have emerged as effective waterproof coatings due to their superior water repellency, which can effectively block water infiltration, making them ideal for long-term waterproofing solutions. As depicted in Figure 6a, a mixed coating primarily consisting of  $\text{SiO}_2$  was successfully deposited onto the surface of polyester fabrics, resulting in a superhydrophobic coating [83]. The fabricated fabrics exhibited remarkable superhydrophobicity, characterized by a water contact angle of  $155.61 \pm 1.42^\circ$ . Notably, the fabricated fabrics also demonstrated exceptional mechanical durability, retaining their superhydrophobicity even after 300 bending and twisting cycles. This remarkable performance underscores the potential of silicon-based materials as robust and long-lasting waterproof coatings for various applications. Meanwhile, carbon-based materials are prevalent inorganic substances utilized in the creation of superhydrophobic coatings. Zhu et al. [84] presented an efficient methodology for creating a superhydrophobic coating using CNTs, as illustrated in Figure 6b. The endowment of surfaces with both strong reusability and effortless repairability represents a novel avenue for prolonging the lifespan of superhydrophobicity, thereby advancing the field of functional coatings. In addition, metal oxides have also been utilized in the development of superhydrophobic coatings. Peng et al. [85] introduced a highly efficient and straightforward method for fabricating stable superhydrophobic surfaces using Al oxide (Figure 6c). This approach involves the rapid formation of a rough hierarchical alumina pyramids-on-pores (HAPOP) surface under room-temperature conditions. Subsequently, the deposition of a modifier, stearic acid (STA), results in the achievement of exceptional non-wetting and extremely

slippery properties. This method offers a promising avenue for the production of durable and functional superhydrophobic coatings with metal oxides.

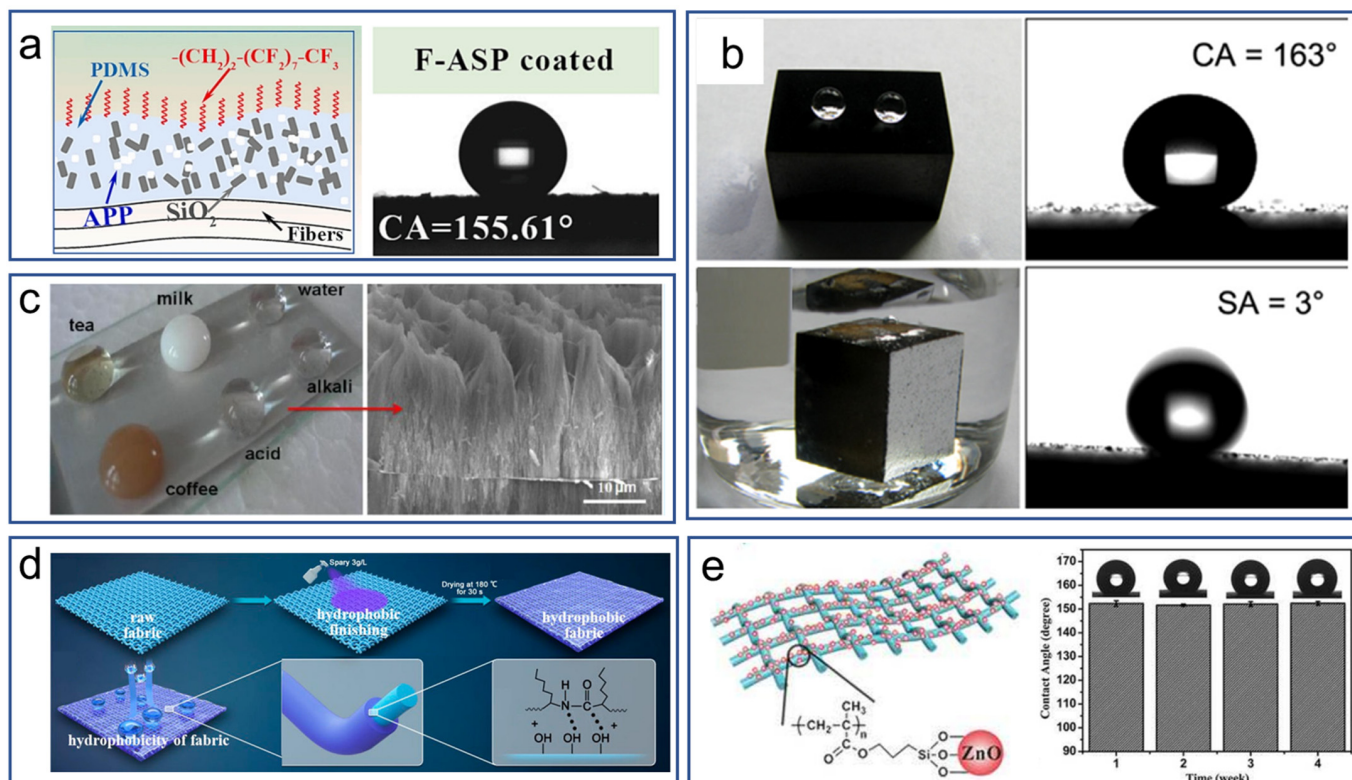


**Figure 6.** Materials utilized for the preparation of superhydrophobic coatings exhibit a diverse range of properties and functionalities: (a) Fabrics possess a superhydrophobic coating based on SiO<sub>2</sub> (reprinted with permission from Ref. [83], copyright 2023 Elsevier); (b) Excellent hydrophobic properties of CNT coating (reprinted with permission from Ref. [84], copyright 2014 Elsevier); (c) Photographs depicting the various liquid droplets present on the PDES-MS surface (reprinted with permission from Ref. [85], copyright 2014 American Chemical Society); (d) Schematic illustration of the preparation of WSiPU-treated hydrophobic fabric (reprinted with permission from Ref. [86], copyright 2023 Elsevier); (e) The long-term superhydrophobicity of the PET-g-PMAPS/ZnO fabric (reprinted with permission from Ref. [87], copyright 2019 Elsevier).

Secondly, organic superhydrophobic coating materials primarily consist of polymeric substances, including polystyrene (PS), polyethylene (PE), polyurethane (PU), etc. Through the implementation of straightforward optimization procedures, it is possible to achieve a satisfactory superhydrophobic effect. Zhang et al. [86] developed a hydrophobic fabric through depositing glyceryl monostearate (GMO)-modified fluorine-free waterborne polyurethane (WPU) emulsion on diverse fabric substrates (Figure 6d). The fabricated fabric exhibited remarkable hydrophobicity, demonstrated through a water contact angle exceeding 140°, along with durable performance, enduring over 50 cycles of abrasion and laundry resistance.

Thirdly, inorganic–organic composite superhydrophobic coating materials hold significant importance in the realm of superhydrophobic coatings. These coatings are fabricated through the deposition of inorganic nanoparticles onto organic polymers, thereby integrating the advantageous properties of both inorganic and organic components. This approach offers a synergistic combination of durability, stability, and hydrophobic performance, making it a highly effective solution for achieving superhydrophobicity. Wu et al. [87] successfully deposited a ZnO layer onto polyethylene terephthalate (PET) fabric through a radiation-induced graft polymerization process. It is worth noting that the fabricated material maintained high superhydrophobicity even after enduring 40 laundering cycles,

as depicted in Figure 6e, demonstrating the excellent stability of the inorganic–organic composite superhydrophobic coating.

With the development of deposition technology, these coating materials can be applied to fibers or textiles using various methods [88], including impregnation, chemical vapor deposition, sol–gel processing, electrospinning, and covalent layer-by-layer assembly.

The impregnation method is a pivotal technique frequently utilized in load preparation, involving dispersing the active component within a solution and subsequently impregnating it onto the carrier material, ensuring its penetration into the internal surface. In the illustration in Figure 7a, the nanoparticles are firmly immobilized on the surface of the cotton fabric, affording superhydrophobicity through the impregnation process. Notably, the treated fabric maintained stable superhydrophobicity even after repeated use for 90 cycles, demonstrating remarkable durability. Furthermore, it exhibited exceptional chemical stability in harsh environments, including strong acidic and alkaline solutions [89].

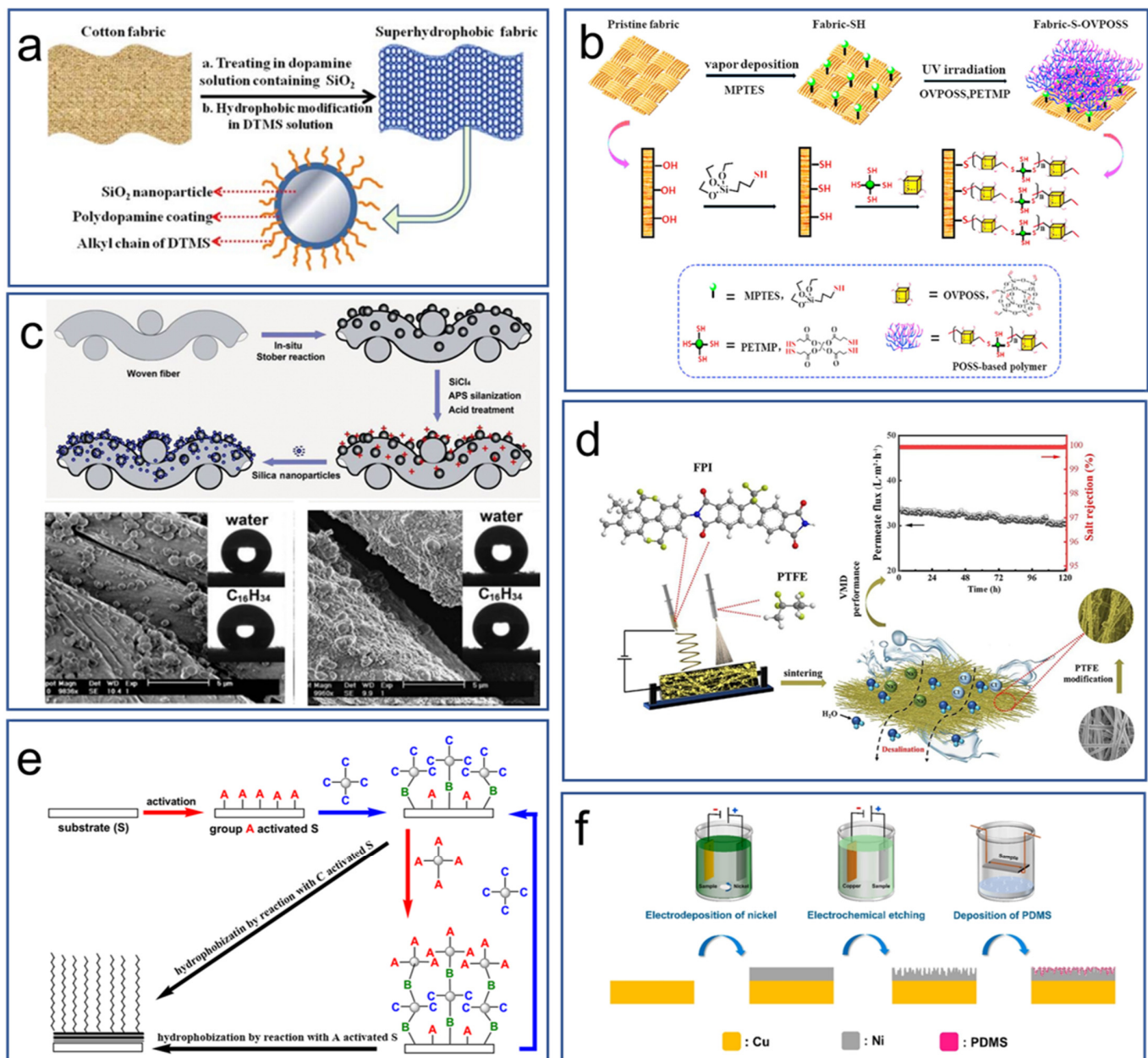


**Figure 7.** Various coating methods are utilized in the production of superhydrophobic coatings: (a) Schematic representation of the preparation of superhydrophobic fabric via dip coating (reprinted

with permission from Ref. [89], copyright 2015 John Wiley & Sons, Inc.); (b) The fabrication process of superhydrophobic fabrics via chemical vapor deposition (reprinted with permission from Ref. [90], copyright 2019 Elsevier); (c) The fabrication process of superhydrophobic fabrics by sol–gel processing (reprinted with permission from Ref. [91], copyright 2009 American Chemical Society); (d) The fabrication process of superhydrophobic fabrics through electrospinning (reprinted with permission from Ref. [92], copyright 2023 American Chemical Society); (e) The fabrication process of superhydrophobic fabrics through covalent layer-by-layer assembly (reprinted with permission from Ref. [93], copyright 2009 Elsevier); (f) Schematic diagram of the fabrication process of a superhydrophobic surface through integration of distinct technologies (reprinted with permission from Ref. [94], copyright 2023 Elsevier).

Chemical vapor deposition (CVD) is an advanced technique used to deposit gaseous reactants onto a substrate, ultimately resulting in the formation of a nonvolatile solid film. The morphology of the resulting film is significantly influenced by the underlying surface morphology of the substrate, which often serves as a template for the deposition process. This technique provides precise control over the composition and structure of the deposited film, enabling the creation of superhydrophobic textile fabrics. Zimmermann et al. [90] employed a single-step gas-phase coating technique modifying fabric fibers with polymers to fabricate superhydrophobic textile fabrics. The deposition of polymers onto the fabric surfaces simultaneously enhanced the surface roughness, thereby imparting exceptional stability against acids, bases, salts, and acetone. Consequently, the fabrics exhibited robust superhydrophobicity, a remarkable property that holds promise for various practical applications.

Sol–gel processing is a prominent technique to prepare superoleophobic textiles, which not only ensures the homogeneity and reproducibility of the material but also enables precise control of surface morphology, thereby conferring exceptional oleophobicity to the textiles. Leng et al. [91] detailed the fabrication of superoleophobic cotton textiles that exhibited multiple length scales via sol–gel processing. This hierarchical roughness was achieved through the meticulous integration of two additional layers of covalently bonded silica particles onto the woven structure, as illustrated in Figure 7c. The sol–gel processing not only enhanced the surface roughness but also provided a stable and durable oleophobic coating, making it an ideal candidate for various practical applications.

Electrospinning is a spinning process that utilizes a polymer liquid to generate a jet flow under the influence of a strong electric field. In recent years, many superhydrophobic surfaces have been fabricated through electrospinning hydrophobic materials onto substrates. As shown in Figure 7d, Huang et al. [92] proposed a hydrophobic membrane developed through the electrospinning of FPI and the double electrospinning of PTFE particles. It was found that the membrane exhibited high superhydrophobicity, with a water contact angle of  $155.3^\circ$ , which was attributed to the membrane's unique rough micro/nano surface structure.

Covalent layer-by-layer assembly offers a versatile platform for the fabrication of thin-film nanocomposites. Its popularity stems from its simplicity and tolerability, enabling the construction of intricate nanostructures with ease. Following the layer-by-layer assembly process, the exterior surface typically harbors residual functional groups (Figure 7e). These residual groups serve as reactive sites for covalent hydrophilization through interaction with low-surface-energy agents [93], thus enhancing the hydrophilic properties of the material.

Furthermore, researchers have explored the integration of distinct technologies to create superhydrophobic fabrics possessing exceptional characteristics. Ye et al. [94] described an approach which combined electrochemical etching and chemical vapor deposition to fabricate a superhydrophobic surface with hierarchical and multi-scale micro/nanostructures, as depicted in Figure 7f. The resulting surface displayed remarkable water repellency, evinced by a high contact angle (CA) of  $158.5 \pm 0.4^\circ$ , thereby demonstrating its exceptional hydrophobic properties. Additionally, the superhydrophobic surface displayed impressive

mechanochemical stability and self-cleaning capabilities, attributes greatly enhancing its potential for practical applications.

### 3.3. Fabricating Technologies for Hydrophobic Smart Fabric-Type Wearable Electronics

The advancement of fabricating technologies for hydrophobic smart wearable electronics is primarily motivated by their diverse functional applications. A significant proportion of research efforts have been dedicated to exploring novel superhydrophobic coating materials that are compatible with smart wearable electronics, with a focus on enhancing wearer comfort, which is critical for outdoor and sports scenarios [95–97].

Firstly, inorganic superhydrophobic coating materials have garnered significant attention. For example, Miao et al. [98] introduced a hydrophobic fabric-based wearable electronics system designed for personalized healthcare applications. That system exhibited superhydrophobic properties due to the unique heterogeneous core–sheath interlocking structure, where AgNWs serve as the core and graphene forms the sheath (Figure 8a). These fabric-based wearable electronics demonstrated remarkable resistance to water, corrosive acids (pH = 1), and alkalis (pH = 13) even under various mechanical stretching conditions.

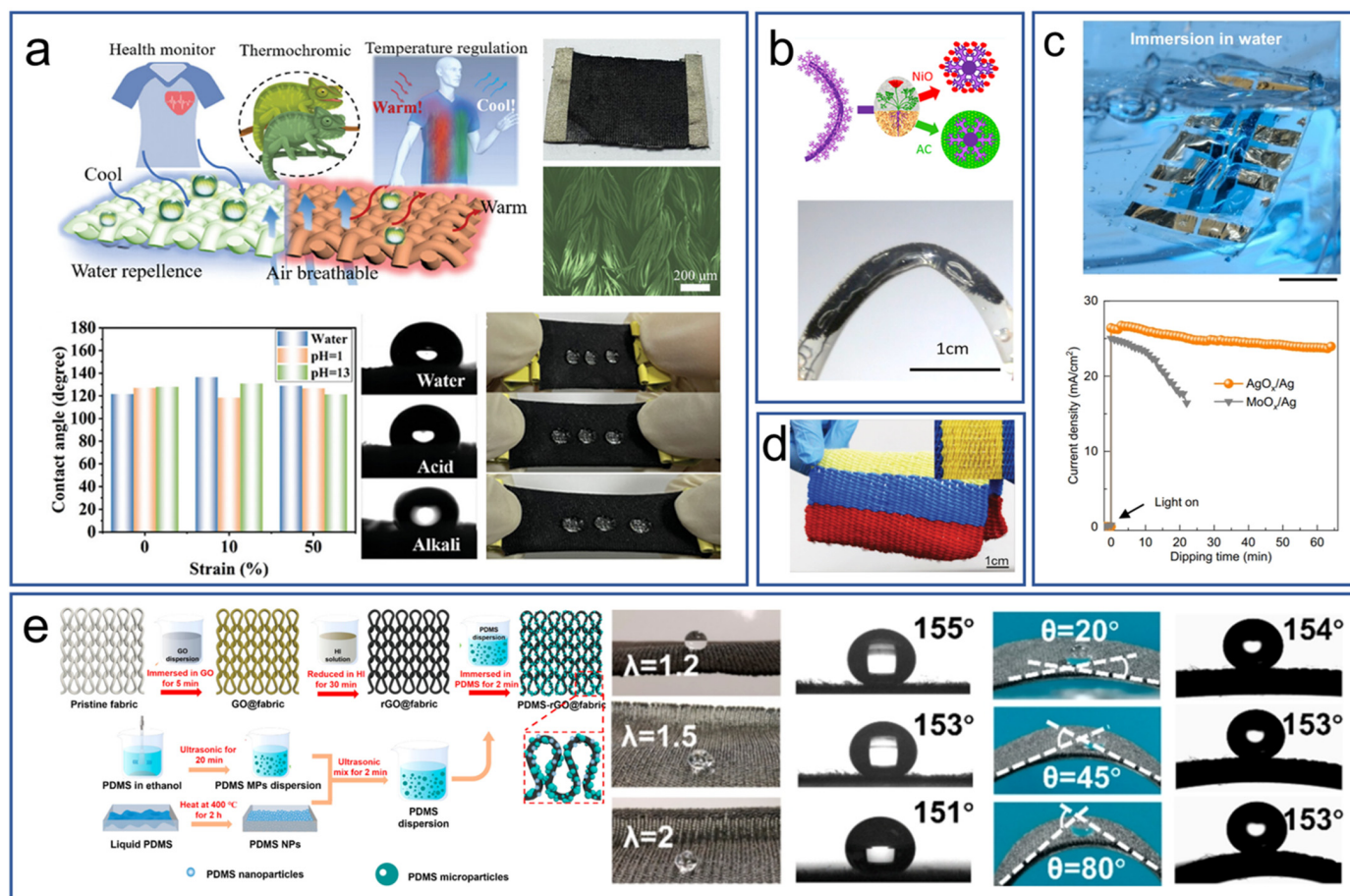


**Figure 8.** Various types of superhydrophobic coatings are utilized in the realm of smart wearable electronics: (a) Construction of a highly elastic smart textile to work stably underwater (reprinted with permission from Ref. [98], copyright 2023 John Wiley & Sons, Inc.); (b) Photograph of a flexible supercapacitor packaged using a plastic tube (reprinted with permission from Ref. [99], copyright 2017 American Chemical Society); (c) Stability of free-standing devices in water (reprinted with permission from Ref. [100], copyright 2024 Springer Nature); (d) Photograph of a photovoltaic textile with remarkable resistance to water (reprinted with permission from Ref. [101], copyright 2016 John Wiley & Sons, Inc.); (e) Schematic illustration of a superhydrophobic conductive fabric (reprinted with permission from Ref. [102], copyright 2022 American Chemical Society).

Secondly, organic superhydrophobic coating materials such as polyvinyl chloride (PVC), polymethyl methacrylate (PMMA), and polydimethylsiloxane (PDMS) have also been extensively employed in the preparation of superhydrophobic coatings. For instance, Fan et al. developed a fiber supercapacitor that exhibited excellent mechanical stability and charge–discharge performance, delivering an energy density of  $0.1408 \text{ mWh}\cdot\text{cm}^{-2}$  [99]. It worked stably under a humid environment, benefitting from being encapsulated in a PVC tube (Figure 8b). These advancements hold significant promise for improving the stability of smart wearable electronics in various practical applications. In addition, Xiong et al. [100] successfully constructed a waterproof and ultra-flexible organic photovoltaic system that was realized through thermal annealing treatment with polyimide (PI), resulting in enhanced waterproofness (Figure 8c). The organic photovoltaics maintained 89% of their original performance after being immersed in water for 4 h. These findings highlight the potential of this approach for developing durable and waterproof organic photovoltaics with excellent mechanical flexibility. Furthermore, Fan et al. [101] proposed an all-solid photovoltaic textile with good waterproof capability which was encapsulated with PMMA (Figure 8d). Moreover, PDMS-based fabrics have received significant attention due to their exceptional waterproof properties. For example, Lai et al. [102] demonstrated a noteworthy approach to fabricating a superhydrophobic fabric-based strain sensor (Figure 8e), achieved through the dip coating of graphene oxide and polydimethylsiloxane micro/nanoparticles, resulting in a water contact angle of  $156^\circ$ . Additionally, the sample exhibited commendable mechanical stability in maintaining its superhydrophobic properties after enduring 300 abrasion cycles. The seamless integration of superhydrophobicity and conductivity within the knitted polyester fabric makes the wireless strain sensor, connected via Bluetooth, a promising option for remote monitoring during aquatic activities such as swimming.

Hydrophobic performance is of utmost importance for smart wearable electronics, as it greatly contributes to their comfortable wearing experience. The hydrophobic properties of these devices are significantly influenced by the selection of hydrophobic coating materials and the associated coating techniques. Given the complexity of this field, it is imperative to adopt a concerted, multidisciplinary approach. With such efforts, swift advancements in the development of waterproof wearable devices that can operate stably under diverse environmental conditions will be achieved in the near future.

#### 4. Air Permeability of Smart Fabric-Type Wearable Electronics

Traditional textiles, while fulfilling basic daily attire requirements, are inadequate in meeting additional functional demands, particularly in terms of air permeability. Prolonged contact between impermeable wearable textiles and human skin has been shown to induce inflammatory responses [103,104]. Consequently, the necessity for wearable textiles to possess superior air permeability is paramount. Such permeability effectively mitigates sweat secretion and retention, maintains skin dryness, and enhances wearer comfort, particularly during summer months.

To this end, researchers have been focusing on enhancing the air permeability of fabric-based wearable electronics through advancements in both textile materials and structures, aiming to optimize the breathability and comfort of these devices while maintaining their electronic functionality. These efforts are essential for the advancement of wearable electronics that are not only functional but also comfortable for users to wear in various environments.

##### 4.1. The Influence of Textile Materials on Air Permeability

It is well known that textile materials hold a crucial position in determining the air permeability of fabrics. Generally, these materials can be categorized into two distinct groups: natural textiles and synthetic textiles [105–107]. The air permeability data of these textile materials were summarized in Table 1. Natural textiles, which encompass cotton, hemp, and wool, are renowned for their inherent superiority in air permeability. However, the availability of these materials is inherently constrained by the natural environment.

Consequently, synthetic textiles have emerged as a viable alternative, offering enhanced air and vapor permeability. These synthetic textiles primarily include nylon, polyester, and acrylic textiles.

**Table 1.** The air permeability data of textile materials (mm/s).

Textile Material	Air Permeability (mm/s)
Cotton textile material	271
Hemp textile material	535
Wool textile material	356
Nylon textile material	255
Polyester textile material	249

The air permeability of natural textiles has been thoroughly investigated. Cotton textiles represent the leading type of natural textiles and are fabricated from cotton yarn; they are commonly referred to as cotton cloth. Cotton textiles boast impressive air permeability, reaching up to 271 mm/s, which contributes to their renowned comfort. Their exceptional breathability ensures that wearers enjoy a comfortable experience, making cotton textiles a preferred material in the realm of wearable electronics.

Hemp textile is another type of natural textile, which is crafted from hemp fibers. While there are numerous varieties of hemp textiles, only a few types of hemp textiles are suitable for practical applications. Among these, ramie stands out as the most widely utilized hemp textile and possess air permeability exceeding 500 mm/s. Its cooling effect and non-stickiness to human skin make it an excellent choice for summer clothing, ensuring a comfortable and breathable wearing experience. Wool textiles constitute a third type of natural textiles, i.e., fabrics constructed primarily from wool fibers. These are renowned for their exceptional air permeability, often exceeding 356 mm/s, which allows excellent breathability. The comfortable wearing experience provided by wool textiles has led to their widespread use in various products, such as woolen cloth. Table 1 presents a comparison of the air permeability of different textile materials, highlighting the hemp textile's superior performance with an air permeability reaching up to 535 mm/s [108]. This demonstrates the potential of natural textiles, particularly hemp and wool, to enhance the air permeability of fabric-based wearable electronics.

The air permeability of synthetic textiles such as nylon textile, polyester textile, and acrylic textile has also been thoroughly investigated [109]. Nylon is a polymer with a linear structure, composed primarily of amide bonds interspersed with methylene groups. Possessing an air permeability of 255 mm/s, nylon textiles exhibit flexibility and wear resistance, thus finding applications in diverse industries such as medical textiles, knitwear, and the silk industry. Polyester textiles demonstrate appreciable air permeability exceeding 249 mm/s. Furthermore, polyester textile excels in shape retention and has been widely utilized in both civilian and industrial textile applications. Acrylic textile is also breathable, but less research has focused on it. As a result, specific data on its breathability remain scarce. Future research should aim to fill this gap and further elucidate the breathability properties of these synthetic textiles.

#### 4.2. The Influence of Textile Structure Design on Air Permeability

The materials used in textiles aside, the structure of textiles also plays a significant role in determining their air permeability [110,111]. The type of structure can greatly influence how air flows through the textile; these structures can be classified into three main categories: woven, knitted, or non-woven structures, as illustrated in Figure 9.



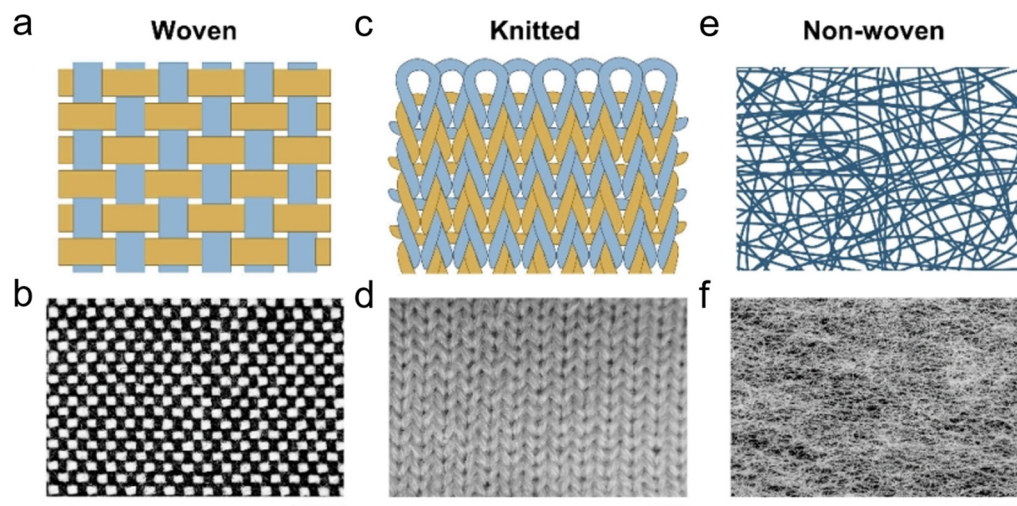


**Figure 9.** The three main structure of textiles of textiles: (a,b) Woven fabric structure, (c,d) Knitted fabric structure; (e,f) Nonwoven fabric structure (reprinted with permission from Ref. [111], copyright 2024 American Chemical Society).

The first type of textile structure is the woven structure, the product of a craft that entails the intricate intertwining of warp and weft yarns on a loom, adhering to a predefined fabric pattern. This process is commonly known as shuttle weaving. Depending on the unique structural qualities of the fabric, woven structures can be further categorized into three distinct types: plain, twill, and satin. Each of these subtypes offers its own set of characteristics, influencing the overall texture, appearance, and functionality of the textile.

Plain weave is fabricated through a regular alternating pattern of longitude and latitude yarns in a 1:1 ratio (Figure 10a). This construction results from the interweaving of warp and weft yarns in an alternating sequence with one up and one down. This interweaving pattern gives the plain textile a high density of interweave points, resulting in a firm texture and a smooth surface. Notably, within the hemp textile category, the plain structure textile exhibited an air permeability of 506 mm/s.

Twill weave is distinguished according to the alternating pattern of longitude and latitude yarns at specific angles (Figure 10b). Compared with the plain weave, twill textiles exhibit a reduced density of longitude and latitude yarns, resulting in a texture that is not as firmly structured as the plain weave. Nevertheless, twill textiles offer a tactile experience that is soft and smooth. Within the realm of hemp textiles, the twill structure demonstrated an air permeability of 535 mm/s.

Satin weave possesses longer alternating longitude and latitude yarns, resulting in a reduced number of interlacing points (Figure 10c). This construction confers a soft texture, a smooth surface, and a lustrous appearance to the satin textile. More importantly, the satin weave exhibited superior air permeability with a value of 677 mm/s within the category of hemp textiles. This exceptional air permeability has contributed to the widespread utilization of satin in various textile applications.

In comparison to twill and satin, the plain texture stands out as the most extensively researched texture in the domain of wearable smart fabrics, owing to its simplicity and straightforwardness in textile construction. For example, Xiao et al. [112] innovatively fabricated an electrothermally responsive fabric by integrating metallic composite yarns with polymeric/thermochromic microcapsule composite fibers, utilizing a melt-spinning technique (Figure 10d). Notably, the resulting advanced wearable smart fabric exhibited remarkable air permeability. Moreover, even with multilayer plain weave construction, the textiles maintained admirable breathability. Cao et al. [113] employed conductive carbon nanotubes (CNTs) and screen-printing technology to develop a wearable smart fabric with a multilayer plain texture structure (Figure 10e). It was found that the wearable smart fabric with a CNT thickness approximating 20  $\mu\text{m}$  demonstrated comparable air permeability to

its traditional counterparts, thus fulfilling the crucial breathability requirements for human skin comfort (Figure 10f). These examples highlight the significant potential of the plain texture in the development of functional and comfortable wearable smart fabrics.

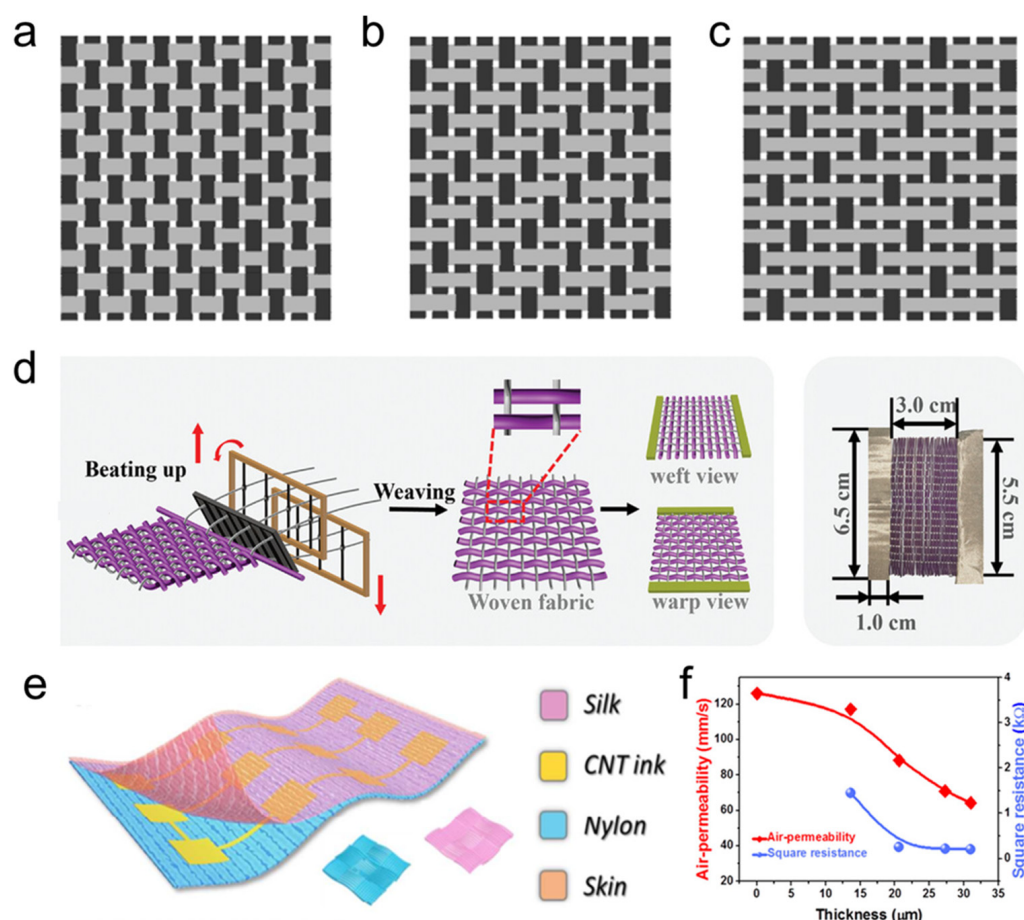


**Figure 10.** The woven structure and its corresponding fabric: (a–c) Plain, twill, satin structure; (d) The preparation process of the multi-responsive fabric (reprinted with permission from Ref. [112], copyright 2023 John Wiley & Sons, Inc.). (e,f) The air permeability of a wearable textile based on a plain weave (reprinted with permission from Ref. [113], copyright 2018 American Chemical Society).

The second type of textile structure is a knitted structure, formed through interlocking loops of yarn to create a fabric. Knitted textiles often have a more open and porous structure than woven textiles, allowing for better air permeability. Depending on the specific method of production, these structures can be further categorized into weft knitting and warp knitting. The fundamental configuration of the knitted structure is clearly depicted in Figure 11a, providing a visual representation of its intricate nature. Knitted textiles, as depicted in Figure 11b, exhibit enhanced air permeability due to their porous coil construction. Zhang et al. [114] reported the development of a breathable wearable textile employing a coated hydrophilic sericin–graphene flake composite. That electronic textile incorporated a meticulously preserved knitted structure, which allowed water vapor to permeate at a rate of  $0.035 \text{ g cm}^{-2} \text{ h}^{-1}$ , suggesting that the well-reserved knitted structure of the textile endowed the textile with good breathability (Figure 11c,d).

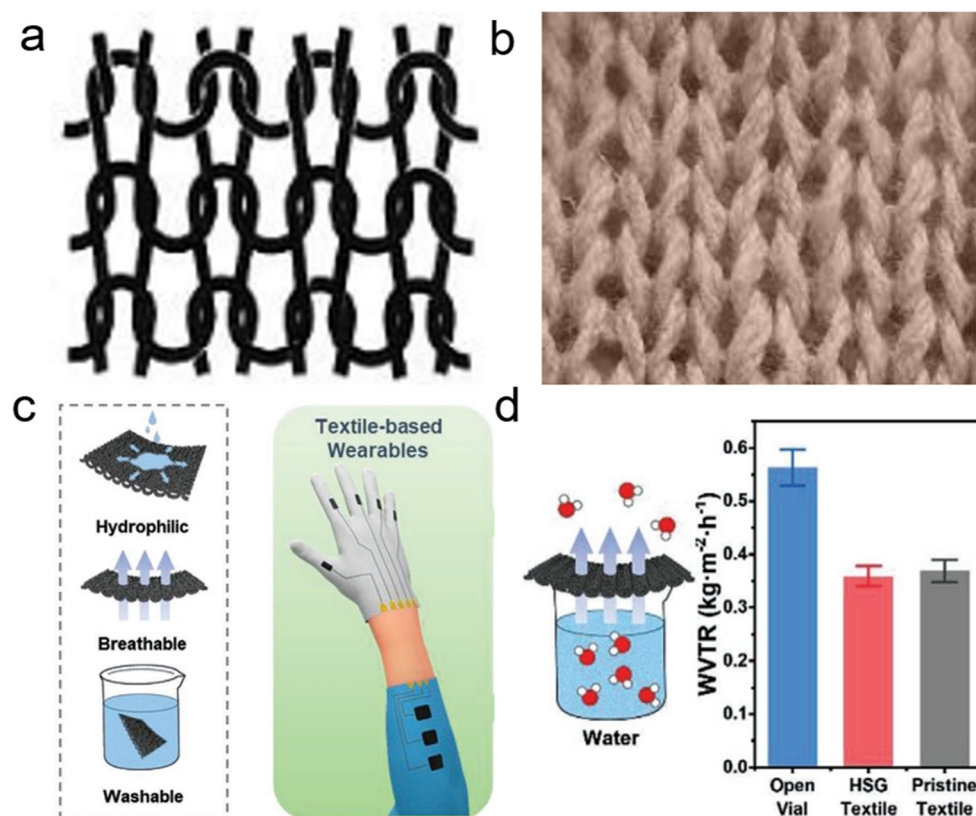


**Figure 11.** The air permeability of knitted textiles: (a,b) The structure of knitted textiles; (c,d) Key features of hexamethylene diisocyanate cross-linked sericin-graphene based knitted textile (reprinted with permission from Ref. [114], copyright 2022 John Wiley & Sons, Inc.).

The third type of textile structure is a non-woven structure, referring to fabrics formed without traditional spinning and weaving processes. The short fibers or filaments are arranged in either an oriented or random manner to create a fibrous network structure. Subsequently, mechanical or thermal bonding or chemical reinforcement techniques are employed to consolidate the structure. For example, Shi et al. [115] introduced a highly flexible nonwoven textile fabricated through a meticulous wet-spinning process that involved hybrid graphene-boron nitride fibers. Subsequently, paraffins were impregnated into the material, resulting in the creation of a unique textile structure, as illustrated in Figure 12a. As a result of this unique fabrication process, the flexible nonwoven composite exhibited an impressive water vapor transmission rate of  $0.00709 \text{ g cm}^{-2} \text{ h}^{-1}$ . This remarkable performance demonstrated its ultrahigh water vapor permeability, rivaling even that of cotton, a naturally occurring material renowned for its breathability.

Beyond the aforementioned structures, researchers have delved into the utilization of embroidered structures encompassing intricate decorative patterns sewn onto the textile substrate using needles and threads. The couching embroidery process involves three key stages. First, a conductive thread carefully follows the specific pattern to start sewing. Secondly, as the sewing progresses, the tension of the thread must be precisely controlled to ensure a smooth and even finish. Thirdly, through the repetition of these embroidery circles, wearable textiles of arbitrary dimensions and patterns can be fabricated. It has been reported that embroidered textiles demonstrate a significant level of air permeability. For example, Huang et al. [70] proposed a wearable energy textile employing an embroidered structure. The resulting energy textile exhibited superior air permeability, allowing the unobstructed passage of gentle winds, as depicted in Figure 12b. It has been found that air permeability can be significantly modulated and optimized to achieve desired performance outcomes via meticulously manipulating the textile materials and structures.

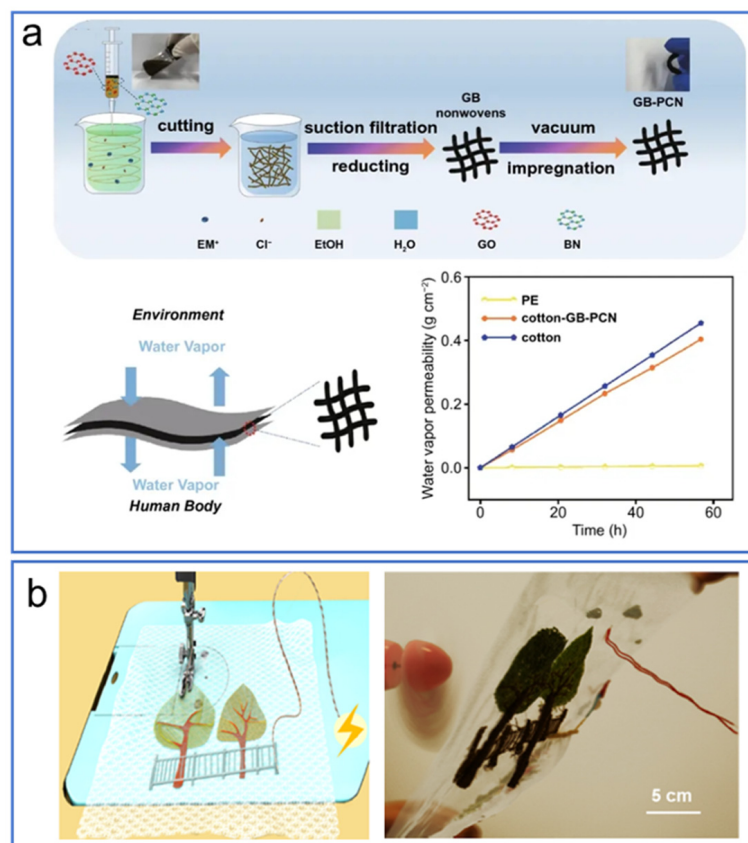


**Figure 12.** (a) The water vapor permeability of a wearable textile with a non-woven structure (reprinted with permission from Ref. [115], copyright 2023 Springer); (b) The water vapor permeability of a wearable textile with an embroidered structure (reprinted with permission from Ref. [70], copyright 2020 Elsevier).

## 5. Endurability of Smart Fabric-Type Wearable Electronics

Despite significant advancements in wearable electronics pertaining to energy efficiency, stretchability, and hydrophobicity, there remains a notable gap in terms of the practical application of smart wearable electronics, particularly relating to their durability under adverse working conditions [116–118]. The potential difficulties and challenges associated with the durability of these wearable electronics have been thoroughly examined under various deformation scenarios, encompassing mechanical stability, chemical stability, and other operational stabilities within complex environments.

### 5.1. Mechanical Stability

In practical applications, wearable electronics are frequently exposed to conditions involving bending, twisting, folding, and other mechanical deformations. These deformations can result in the detachment of conductive materials from their substrate or the breakage of the wearable device itself, significantly compromising the materials' stability and longevity. The design and construction of smart wearable electronics must take into account the requirements for mechanical stability to ensure optimal performance and user satisfaction. Researchers have thus conducted investigations into the impact of these conditions on the performance of wearable electronics, as follows.

Addressing the aspect of bending, Fan et al. [101] proposed a photovoltaic textile incorporating various knitting patterns. Notably, the textile maintained exceptional performance even when bent at an angle of 120° (Figure 13a). In addition, the bending cycle has also been investigated. The electronic textile developed by Peng et al. [119] exhibited a marginal increase in resistance during the initial 1000 to 2000 bending cycles, subsequently

maintaining a stable resistance. These findings indicate that the proposed electronic textile possesses superior flexibility and mechanical durability (Figure 13b).

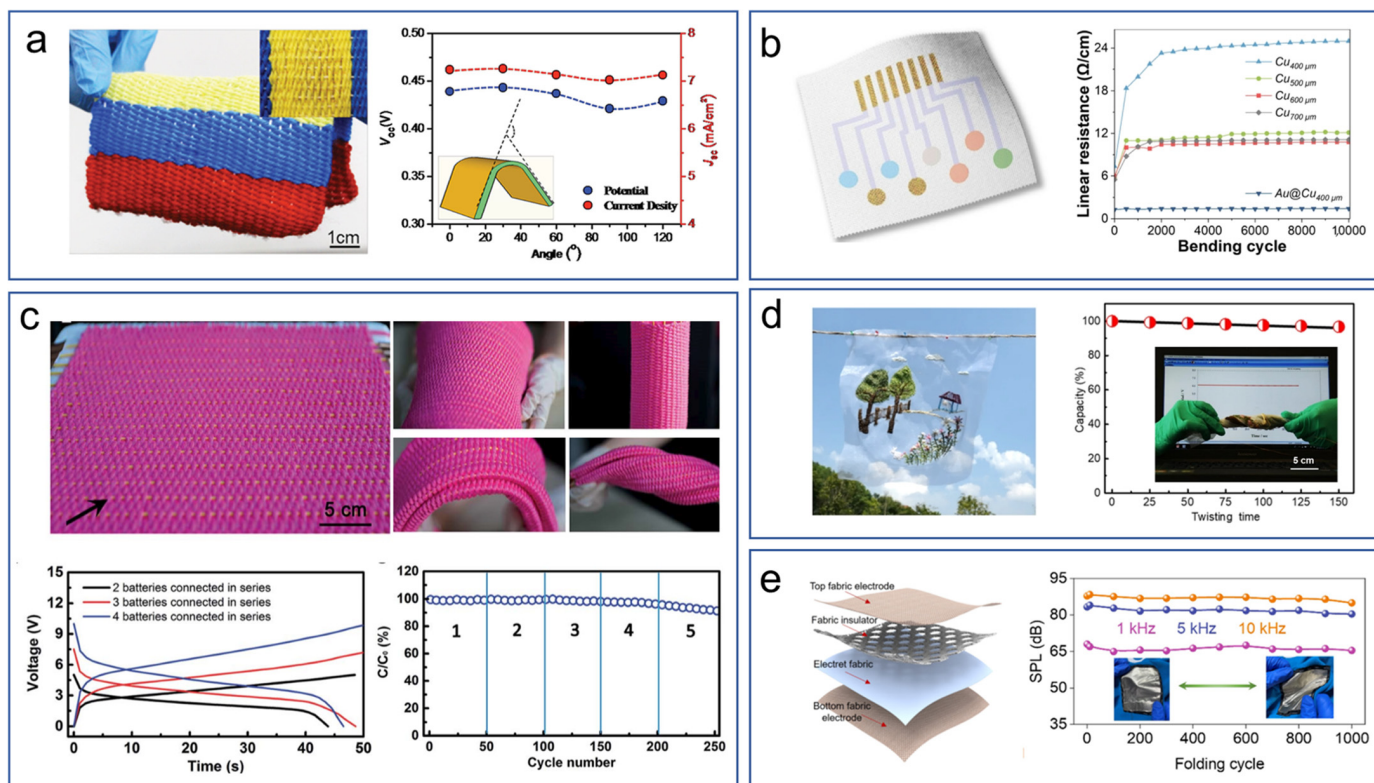


**Figure 13.** Mechanical stability testing of flexible wearable electronics: (a) Stable performance of a photovoltaic textile under various bending angles (reprinted with permission from Ref. [101], copyright 2016 John Wiley & Sons, Inc.); (b) The stability of the smart fabric during the 10,000-cycle bending test (reprinted with permission from Ref. [119], copyright 2024 Springer Nature); (c) Stable performance of an energy textile under various mechanical deformations (reprinted with permission from Ref. [120], copyright 2016 The Royal Society of Chemistry); (d) Stable performance of flexible energy fabric under different twisting times (reprinted with permission from Ref. [70], copyright 2020 Elsevier); (e) Stable performance of fabricated wearable electrostatic transducers under folding conditions (reprinted with permission from Ref. [121], copyright 2024 John Wiley & Sons, Inc.).

In relation to aspects of twisting, Zhang et al. [120] fabricated a fiber-type battery that utilized a polyimide/carbon nanotube hybrid fiber as the anode and a  $\text{LiMn}_2\text{O}_4$ /carbon nanotube hybrid fiber as the cathode, offering a unique and efficient solution for power storage and delivery in twisted configurations. The innovative design allows the battery to be seamlessly integrated into the textile, enabling the material to be folded and twisted into diverse configurations while maintaining electrochemical performance across a range of deformations (Figure 13c). Furthermore, an investigation into bending cycles was conducted. Fan et al. [70] demonstrated a wearable fabric which retained its capacity virtually unchanged after enduring over 100 consecutive twisting cycles, in testament to its resilience (Figure 13d). This lightweight, highly flexible, and soft energy textile represents a groundbreaking advancement in wearable energy storage solutions.

Regarding folding, Zhong et al. [121] fabricated a lightweight and textile-integrated dual-functional electrostatic transducer (ET) that consisted of fabric insulator and electret fabric sandwiched between fabric electrodes (Figure 13e). It was found that the sound pressure level amplitude had small variation at 1, 5, and 10 kHz after continuously folding the ET 1000 times, verifying the mechanical robustness of the ET. Furthermore, it found that the discharge capacity was hardly influenced by folding into different shapes.

Extensive research has been conducted on the stability of fabric-based wearable electronics, with testing particularly focusing on their resilience against diverse mechanical deformations. Looking ahead, these intelligent fabrics will undergo increasingly rigorous testing procedures designed to mimic real-world conditions. Such rigorous testing will lay a solid foundation for their seamless integration into daily life, thereby guaranteeing optimal comfort during wear. This will pave the way for a new era where wearable technology not only performs its functions well but also feels as natural and comfortable as conventional clothing.

### 5.2. Chemical Stability

In addition to mechanical stability, the chemical stability of wearable electronics remains a crucial concern that requires urgent attention [122,123]. Compromises in chemical stability can lead to degradation of performance during the operational processes of devices, and in severe cases, may even result in the release of harmful substances, posing a potential risk to human health. Consequently, chemical stability holds significant implications for both the wearing experience and safety. Currently, the chemical stability of energy devices is primarily evaluated based on factors such as the number of cycles and the duration of performance retention.

Addressing the issue of cycle numbers, Fan et al. [124] conducted rigorous experiments to assess the chemical stability of fiber-shaped supercapacitors (FSCs) (Figure 14a). It was found that even after 10,000 cycles, the fiber-shaped supercapacitor maintained a high areal capacitance of  $3.2 \text{ F cm}^{-2}$ , indicating its superior durability and stability under prolonged use. The findings provide valuable insights into the long-term performance of FSCs and lay the groundwork for their potential application in wearable electronics. Numerous researchers have examined the cycle number stability of fabric-type wearable devices. Zhang et al. [125] proposed fabric-based wearable batteries that demonstrated Coulombic efficiency approaching 100% after 1500 cycles at a current density of  $0.4 \text{ A}\cdot\text{cm}^{-3}$  (Figure 14b). This significant finding underscores the potential of fabric-type wearable devices to maintain stable performance over extended periods of use.

Regarding the duration of performance retention, Peng et al. [126] conducted an investigation into the chemical stability of display textiles. It was found that the electrical resistance of polyurethane ionic gel fibers in the display textiles remained stable in the open air at room temperature ( $\sim 25 \text{ }^\circ\text{C}$ ), without the need for sealing, over a period of 16 days (Figure 14c). Furthermore, Fan et al. [127] assessed the long-term performance of a flexible energy textile (Figure 14d). It was discovered that the fabric possessed the remarkable capability to achieve a charge of up to 6.4 V under ambient solar irradiation, demonstrating its high photovoltaic efficiency. Notably, the flexible energy textile exhibited remarkable air stability, as evidenced by experimental results indicating that the energy textile retained its voltage with minimal loss for over 60 days under ambient conditions. After being charged with solar light, the flexible energy fabric exhibited the capacity to directly power a cell phone, thereby demonstrating its practical utility and viability for real-world applications, representing a significant advancement in the field of wearable technology.

The development of smart wearable electronics that possess exceptional chemical stability is imperative. To enhance their durability, including resistance to oxidation and corrosion, and functionality under complex environmental conditions, it is crucial to adopt appropriate protective measures such as surface passivation. Surface passivation techniques effectively shield the electronic components from harmful chemical reactions, thereby extending their lifespan and maintaining optimal performance. Incorporating these advancements will help to create smart wearable electronics that are not only highly functional but also resilient in various challenging environments.

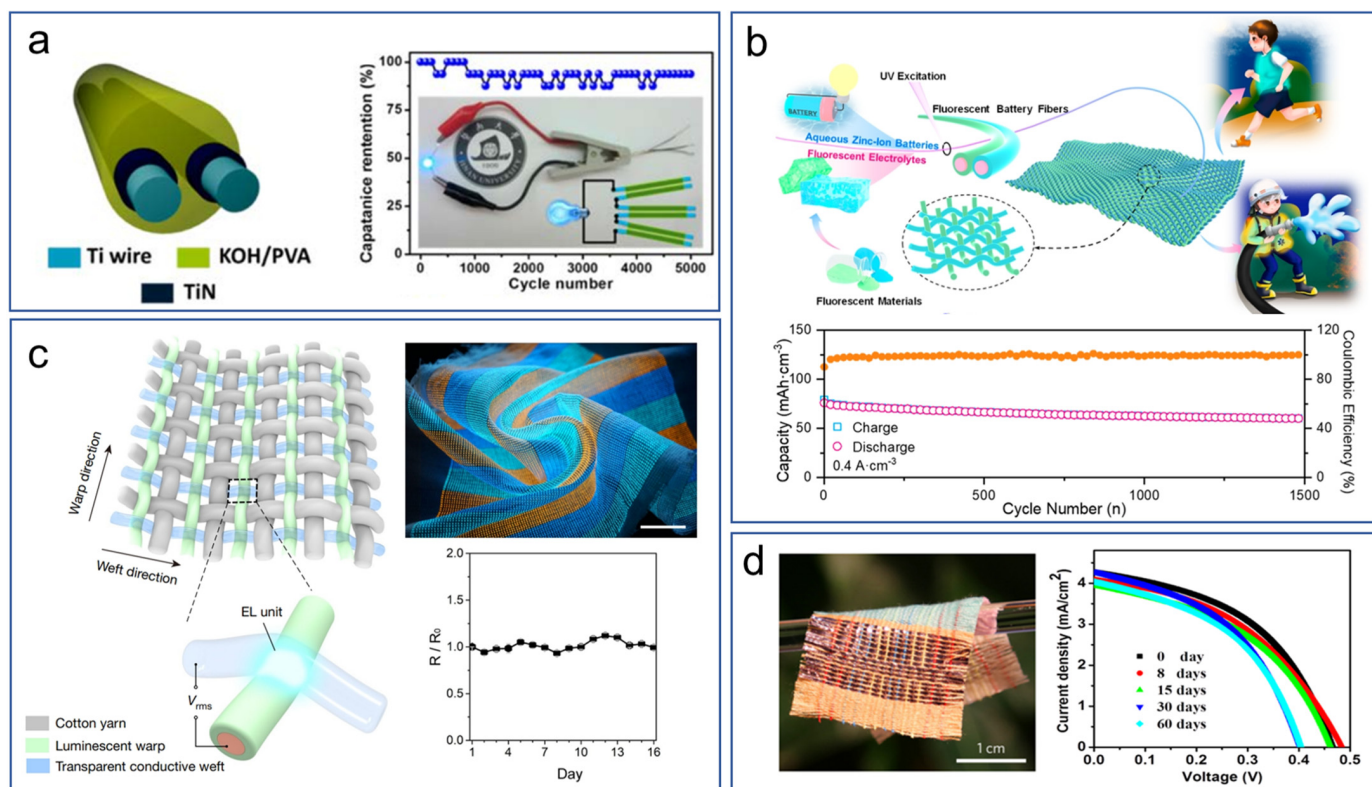


**Figure 14.** The chemical stability testing of smart wearable electronics: (a) Cycling stability of an FSC (reprinted with permission from Ref. [124], copyright 2016 American Chemical Society); (b) Cycling stability of fluorescent battery textiles (reprinted with permission from Ref. [125], copyright 2023 American Chemical Society); (c) Variation of electrical resistance of polyurethane ionic gel fiber in open air at room temperature (reprinted with permission from Ref. [126], copyright 2021 Springer Nature); (d) The duration of performance of the flexible energy textile (reprinted with permission from Ref. [127], copyright 2016 Springer Nature).

### 5.3. Other Working Stability under Complicate Environment

It is worth noting that the stable performance of smart wearable electronics is susceptible to various environmental factors, including temperature, humidity, pressure, etc. [128,129]. When the environmental conditions exceed tolerable limits for the energy device, the stable performance of these electronics can rapidly deteriorate. Therefore, it is crucial to conduct comprehensive investigations into the impact of diverse working environmental conditions, ranging from low to high temperatures and varying pressure levels, on the stable performance of smart wearable electronics. Such rigorous testing is essential to ensure the reliability and durability of these devices in real-world applications, thereby enabling their seamless integration into daily life.

Firstly, in terms of testing under low temperature conditions, Zhi et al. [130] reported a comprehensive study on a flexible zinc manganese-dioxide battery (Zn-MnO<sub>2</sub>-B). It demonstrated remarkable stable cycling performance and exceptional flexibility even under low temperature conditions (Figure 15a). These advantageous characteristics were attributed to the anti-freezing hydrogel electrolyte, offering valuable insights into the design and optimization of smart wearable electronics for cold environments.

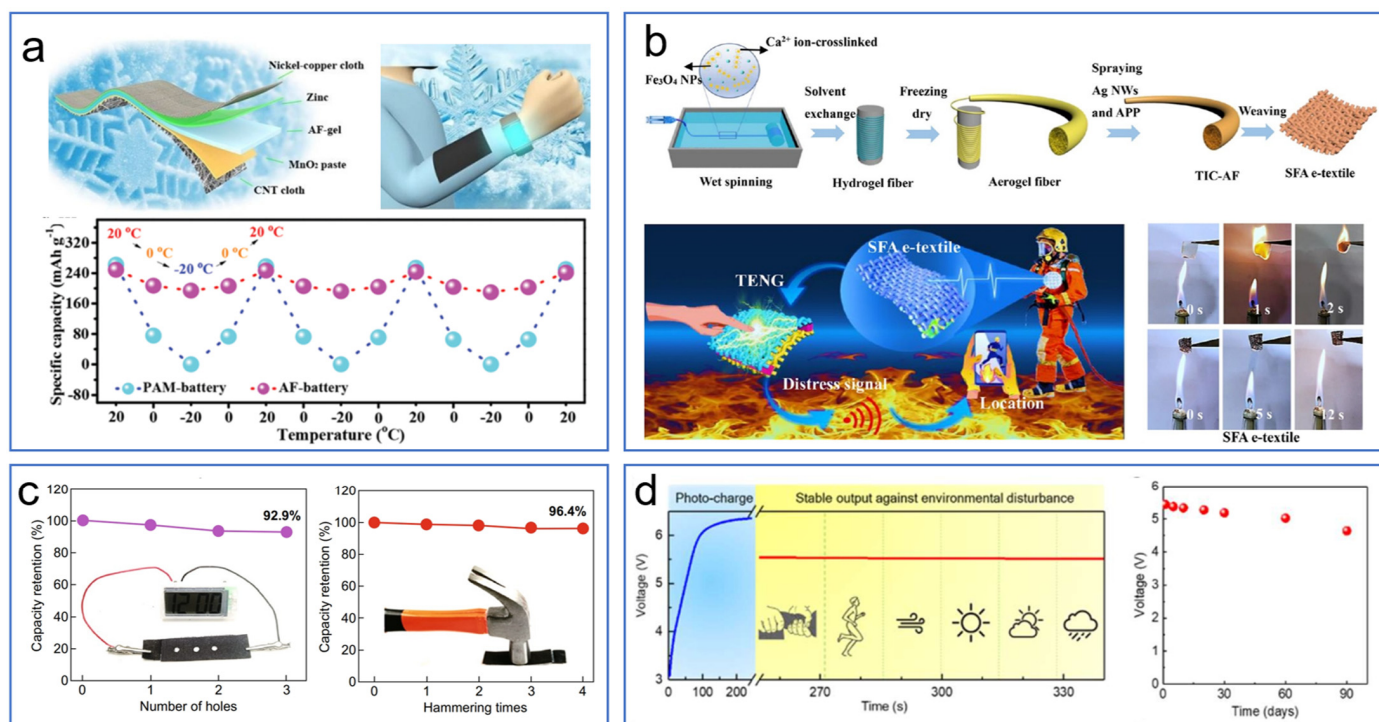


**Figure 15.** The stability of smart wearable electronics under complicate environmental conditions: (a) Cyclic testing of a PAM battery under various temperature conditions (reprinted with permission from Ref. [130], copyright 2019 The Royal Society of Chemistry); (b) Fireproof testing of an SFA e-textile under an alcohol lamp flame (reprinted with permission from Ref. [131], Copyright 2022 American Chemical Society); (c) Electrochemical performance of a zinc-ion battery (ZIB) after hammering and punching tests (reprinted with permission from Ref. [132], copyright 2020 Springer). (d) Stability of a flexible energy textile under various outdoor conditions (reprinted with permission from Ref. [122], copyright 2020 Elsevier).

Secondly, regarding high temperature conditions, Wang et al. [131] conducted a test on a highly safe flexible electronic textile which possessed fireproof properties (Figure 15b). The flexible electronic textile demonstrated significant resistance to ignition within a brief time-frame during the vertical burning test. Furthermore, it exhibited rapid self-extinguishing characteristics once removed from the flame source, underscoring its superior fire-safety performance. That study offers valuable insights into the development of fire-resistant flexible electronic textiles for use in high-temperature environments.

Thirdly, given the stringent safety demands of flexible wearable electronics, it is imperative to simulate various harsh environments, encompassing hammering and stamping, to rigorously assess their stability. This comprehensive testing ensures that these devices can withstand rigorous conditions and maintain their integrity, thus meeting the rigorous safety standards required for practical applications. Huang et al. [132] conducted a rigorous investigation into the performance of a ZIB under destructive conditions, simulating harsh environments. After subjecting the ZIB to five consecutive hammering cycles, with an estimated external force of at least 26.3 kPa, the flexible wearable battery exhibited a remarkable capacity retention of 96.4%. In addition, the flexible wearable battery's resilience was tested by drilling holes in it. Notably, even after three holes were punched, it also maintained a high capacity retention of 92.9% (Figure 15c). These findings suggest that ZIBs offer a promising new avenue for flexible and wearable energy storage technologies, being capable of enduring severe mechanical stresses while maintaining superior electrochemical performance.

Fourthly, Fan et al. [122] reported an outdoor test on a flexible photo-rechargeable energy fabric. The testing conducted under outdoor conditions validated its suitability



for real-world applications, highlighting the potential of such innovative materials in the field of wearable electronics, particularly during summer months (Figure 15d). This innovative material holds promise for expanding the realm of wearable technology and energy harvesting in outdoor environments.

The consistent and reliable performance of smart wearable electronics must be meticulously evaluated prior to their integration into daily life. The stability of an energy device is fundamentally influenced by various factors. Regarding mechanical stability, rigorous testing methods have been employed to assess the stable performance of smart wearable electronics, encompassing bending, twisting, and folding. Chemical stability was primarily quantified through the number of cycles and the duration of performance retention exhibited by energy devices. Additionally, the operational stability of these electronics has been evaluated under challenging environments, such as high-and low-temperature conditions, as well as under varying pressure environments. Through thoroughly assessing stability from all these perspectives, it is anticipated that smart wearable electronics will not only significantly extend the lifespans of devices but also mitigate any potential risks prior to their application in practical scenarios.

## 6. Color-Change Ability of Smart Fabric-Type Wearable Electronics

Smart color-changeable textiles, as an emerging research avenue in wearable technology, are attracting considerable academic and industrial attention due to their profound implications in diverse applications encompassing non-emitting displays, sensing technologies, military camouflage systems, optical recording mechanisms, environmental monitoring platforms, and stealth operations [133–136]. These textiles exhibit remarkable color variations in response to external stimuli, including electrical, optical, and thermal factors. The fundamental mechanism behind this phenomenon lies in the alteration of the molecular structure of the color-changing material coating the fabric surface, which subsequently modifies its light absorption peak, ultimately leading to a discernible color shift, which can be categorized into three primary types according to the principles of color change: electrochromic, photochromic, and thermochromic textiles.

Electrochromic textiles include those exhibiting reversible alterations in their optical characteristics, specifically reflectivity, transmittance, and absorptivity, when an electric field is applied. Photochromic textiles, on the other hand, undergo color transitions in response to exposure to light of varying wavelengths. Thermochromic textiles refer to textiles that exhibit color variations when subjected to changes in temperature, either through heating or cooling [137]. In essence, the color-changing capacity of these textiles is predominantly influenced by the color-changeable materials employed, which are discussed as follows.

### 6.1. Color-Changeable Materials

As we know, according to the varying stimulus sources, there exist three distinct types of color-changeable materials: electrochromic materials, photochromic materials, and thermochromic materials.

Firstly, there are two types of electrochromic materials: inorganic and organic. Inorganic electrochromic materials can be further classified as anodic or cathodic color-changing materials. Anodic color-changing materials, such as NiO, MnO<sub>2</sub>, and Co<sub>3</sub>O<sub>4</sub>, exhibit a colorless state at low valence, whereas they undergo a color change in their high-valence state [138]. Conversely, cathodic color-changing materials, such as WO<sub>3</sub>, MoO<sub>3</sub>, TiO<sub>2</sub>, and Nb<sub>2</sub>O<sub>5</sub>, are colorless in their high-valence state and undergo a color change in their low-valence state [139]. As a typical example, WO<sub>3</sub> thin film is an early and extensively prototypical electrode coloring material. Lee et al. [140] demonstrated a type of m-WO<sub>3-x</sub> NW film exhibiting remarkable dual-band electrochromic performance, characterized by high coloration efficiency and excellent cycle stability (Figure 16a). Regarding organic electrochromic materials, these mainly include conjugated polymers, organic small molecules, and metal organic chelates. Among these, conjugated polymer (CP) electrochromic ma-

materials stand out for their rich color palette, high color contrast, swift response time, and exceptional flexibility. The doping/dedoping process of ions within conjugated polymers induces reversible color conversions. The conjugated polymers commonly employed for electrochromism include polyaniline (PANI), polythiophene, and polypyrrole [141].

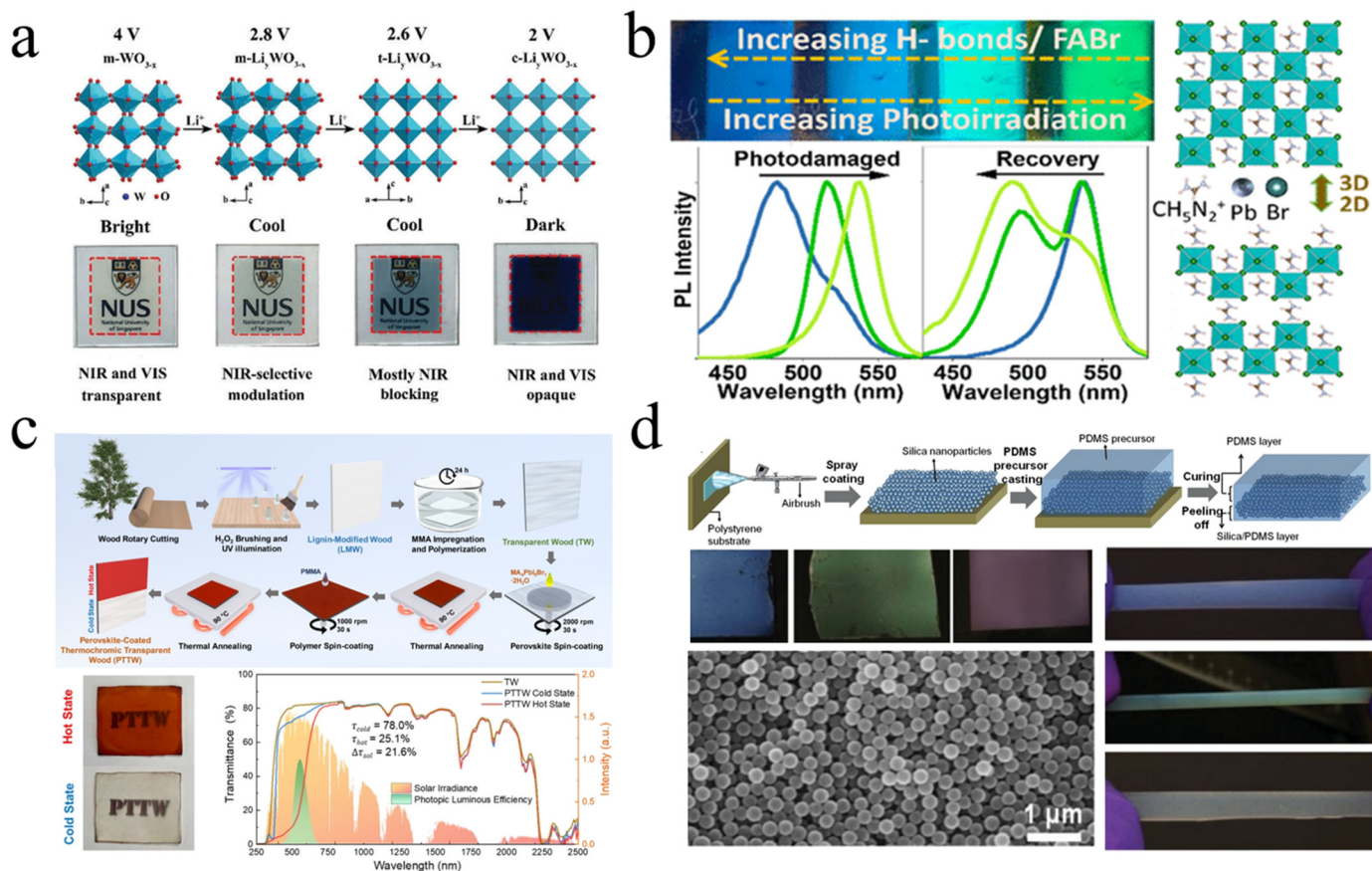


**Figure 16.** Various types of color-changeable materials. (a) Electrochromic material based on  $WO_{3-x}$  nanowires and its underlying mechanism (reprinted with permission from Ref. [140], copyright 2018 The Royal Society of Chemistry); (b) Photochromic material based on oriented layered halide perovskite and its photochromic ability (reprinted with permission from Ref. [142], copyright 2022 American Chemical Society); (c) The structure and working principle of a perovskite-coated thermochromic transparent device (reprinted with permission from Ref. [143], copyright 2023 The Royal Society of Chemistry); (d) The fabrication process of the stress-induced material and its digital photographs (reprinted with permission from Ref. [144], copyright 2015 John Wiley & Sons, Inc.).

Secondly, photochromic materials are classified into inorganic and organic types. Inorganic photochromic materials mainly include transition metal oxides, polyoxometalates, and metal halides. Among these, metal halide photochromic materials (e.g.,  $CuCl_2$ ,  $CdCl_2$ ,  $AgX$ ) stand out for their good thermal stability and long color-change duration. Kang et al. [142] proposed a photochromic hydrogel comprising silver bromide and cuprous bromide. This hydrogel possesses the remarkable ability to undergo reversible changes in color, shifting seamlessly between a light blue hue and a brown tint when exposed to air (Figure 16b). It has potential application prospects in the field of intelligent materials such as photochromic contact lenses, sensors, artificial intelligence devices, or bionic skin. Meanwhile, organic photochromic materials mainly include spiropyran, arginine anhydride, diarylethylene, and azobenzene, which have advantages such as modifiable molecular structures, high color-changing efficiency, and bright colors. Among these, spiropyran has been the most widely studied organic photochromic material. Abdollahi et al. developed a novel functionalized stimulus-responsive emulsion particle containing spiropyran

(1 wt.%) through semi-continuous emulsifier-free emulsion polymerization. This functionalized emulsion particle can be employed as an anti-counterfeiting ink for writing on cellulose paper. The written text exhibits a purple hue upon irradiation with ultraviolet light (365 nm) for 1 min and subsequently fades into a colorless state upon exposure to visible light.

Thirdly, thermochromic materials can be also classified into inorganic and organic types. The inorganic thermochromic materials mainly include metal oxides and metal iodides such as CuI, PbO, Hg<sub>4</sub>HgI<sub>4</sub>, Fe<sub>2</sub>O<sub>3</sub>, and VO<sub>2</sub>, which exhibit exceptional temperature resistance and durability. Du et al. [143] proposed a perovskite-coated thermochromic device which was developed through spin coating the perovskite material MA<sub>4</sub>PbI<sub>5</sub>Br<sub>1</sub>·2H<sub>2</sub>O onto a treated transparent wood substrate, achieving effective solar modulation and thermal management (Figure 16c). Organic thermochromic materials mainly include conjugated polymers, hydrogels, liquid crystals, which have the advantages of rich colors, low color-change temperature, high color-change sensitivity, etc. Among these, conjugated polymers such as polydiacetylene (PDA) are a widely studied type of thermochromic polymers. For example, Peng et al. [145] fabricated a thermochromic device based on PDA showing great potential in various fields such as aerospace and sensors.

In addition to the aforementioned intelligent color-changing materials, various other types have been discovered. In the existing research, solvents, magnets, forces, gases, and other stimuli have been reported to act as excitation sources, triggering color changes. For example, Yang et al. [144] fabricated a composite film that consisted of a thin layer of quasi-amorphous silica NPs seamlessly embedded within a robust elastomeric PDMS matrix. Initially, this film exhibited remarkable transparency, achieving transmittance levels exceeding 90% in the visible wavelength range, while maintaining a constant color even under increasing strain. However, upon mechanical stretching, the transmittance underwent a significant reduction to 30%, revealing a distinct structural color that was angle-independent at strains exceeding 40% (Figure 16d). This innovative material demonstrates the potential for creating tunable optical properties through the controlled manipulation of nanostructured components within an elastomeric matrix, offering promising applications in the field of flexible wearable optical devices and strain sensors.

Regarding color-changing materials, the stability and durability of these materials remain concerning, as they often experience degradation in color performance over time or under varying environmental conditions. Furthermore, the response speed and reversibility of the color change are limited, preventing rapid or continuous color variations. Additionally, the production costs of some advanced color-changing materials can be prohibitively high, limiting their widespread commercialization.

## 6.2. Color-Changeable Textiles

Color-changeable textiles hold significant potential for application in various aspects of daily life, including non-emitting displays, sensors, military camouflage, ornaments, and beyond [146–151]. Nevertheless, the realization of this potential is hindered by several challenges. On the one hand, there is a pressing need for scalable encapsulation technologies that can effectively prevent electrolyte leakage while preserving the advantages of fiber-shaped or interwoven substrates. On the other hand, some color-changeable materials exhibit irreversible or sluggish color transitions in response to electrical stimuli. Considerable research efforts have been directed toward addressing these issues. This includes the exploration of all-solid color-changeable textiles through the development of novel solid-type electrolytes, aimed at facilitating the encapsulation process. Additionally, diverse color-changeable materials and their color-changing mechanisms have been investigated and optimized to achieve textiles with excellent optical quality, rapid color conversion, and robust reversibility of color changes [152–154].

Firstly, electrochromic textiles have the advantages of high controllability, low energy consumption, and rich variety of materials and color changes, thus providing a good strategy for achieving intelligent color change. For example, Invernale et al. [155] developed

an electrochromic textile through spray-casting an electrochromic precursor onto one side of a conductive spandex substrate. This electrochromic textile was able to exhibit two colors of red and blue, which were triggered by the varying redox states of the electrochromic polymer. Impressively, the electrochromic textile's transition time between colors was as swift as 0.3 s (Figure 17a).

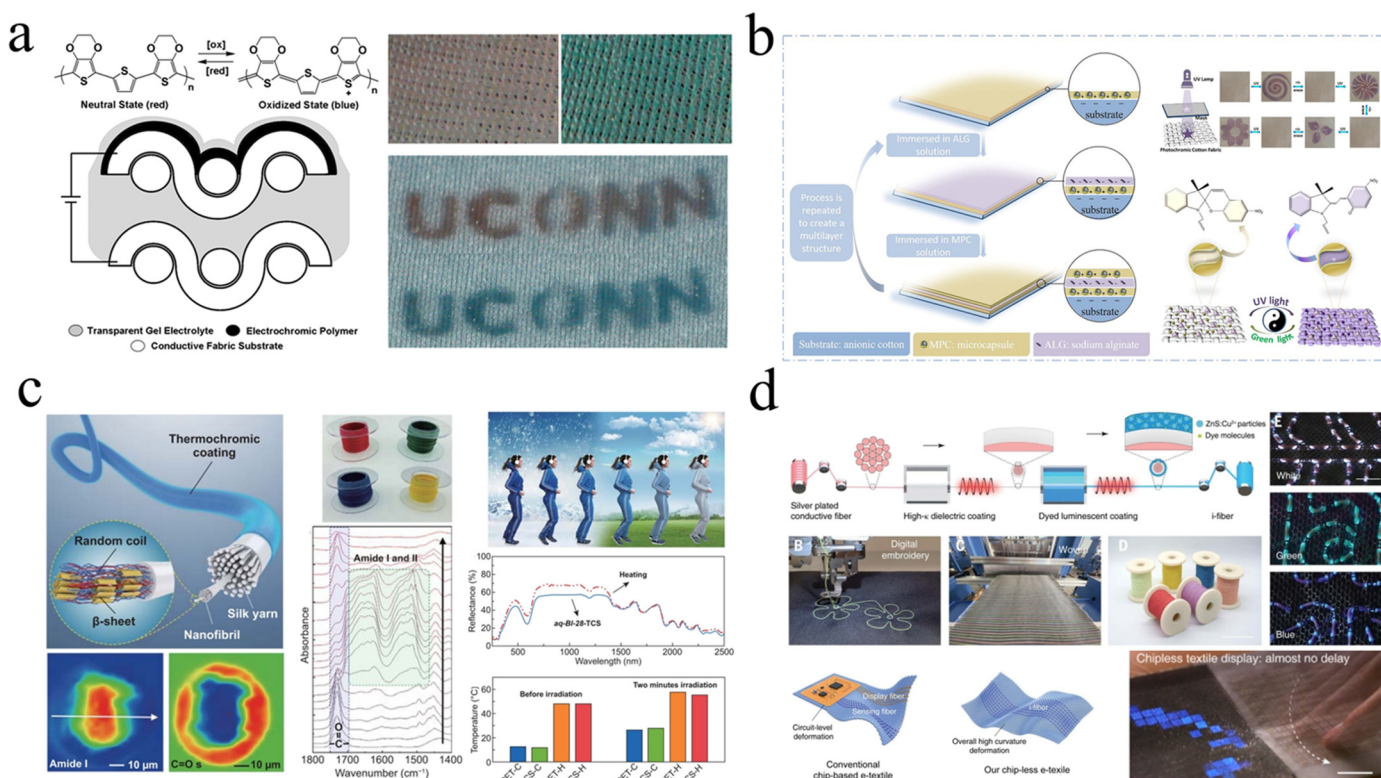


**Figure 17.** Color-changing textiles. (a) Stretched electrochromic spandex textile electrode in different states (reprinted with permission from Ref. [155], copyright 2010 American Chemical Society). (b) Photochromic fabric and its photochromic mechanism (reprinted with permission from Ref. [156], copyright 2020 The Royal Society of Chemistry). (c) Spinning, structures, and properties of thermochromic textiles (reprinted with permission from Ref. [157], copyright 2021 Springer). (d) The design of body-coupled interactive color-changing textiles (reprinted with permission from Ref. [158], copyright 2024 The National Academy of Sciences of the USA).

Secondly, photochromic textiles possess significant potential for diverse applications due to their ability to undergo reversible color changes in response to light irradiation. As an illustrative example, He et al. [156] created a novel photochromic cotton fabric through the employment of a layer-by-layer self-assembly technique (Figure 17b). The innovative fabric exhibited remarkable color-changing capabilities, transitioning from colorless to purple within a mere 12 s under UV light. Furthermore, the fabric maintained a photochromic performance retention rate of 94.65% even after over 20 cycles.

Thirdly, thermochromic textiles have garnered significant interest due to their straightforward preparation methods, cost-effectiveness, and broad applicability. For instance, Ling et al. [157] introduced a thermochromic textile fabricated through spinning and continuous coating techniques, which exhibited robust hydrophobicity, rapid programmable thermochromic response, and excellent cycling performance (Figure 17c). Furthermore, the utilization of these thermochromic fabrics for temperature regulation was effectively demonstrated, thereby confirming their immense potential in the realm of human-machine interfaces.

Notably, with the advancement of technology, the use of electromagnetic energy dispersed in the environment as a wireless driving force for fiber to change its color has attracted attention. Yang et al. [158] developed a color-changing textile able to use

the interactive object itself—the human body—to couple the ambient electromagnetic environment energy. This approach enables preparation of innovative color-changeable textiles meeting the rigorous demands of diverse domains, such as non-emitting displays, sensors, and military camouflage, aptly demonstrating the extensive applicability of this technology in the realm of wearable electronics and smart clothing.

The emergence of smart color-changing fabrics offers unprecedented versatility and adaptability, allowing them to dynamically adjust their color in response to environmental stimuli or user interaction, which can enhance user experiences, provide visual cues, and even communicate information in a unique and engaging way. In order to ensure that the fabric retains its function under different conditions, a combination of complex material science principles and advanced manufacturing techniques is required. Additionally, the fabric may exhibit diverse characteristics in response to varying stimuli, necessitating meticulous calibration of the system to achieve the desired effects. This calibration process can be challenging and requires a thorough understanding of the material's properties and the interactions between the fabric and its environment.

## 7. Discussion and Prospects

This review provides a comprehensive overview of smart fabric-based wearable electronics design toward comfortable wearing, in which key factors such as stretchability, hydrophobicity, air permeability, color-changing capabilities, and durability are highly demanded, as summarized in Figure 18.

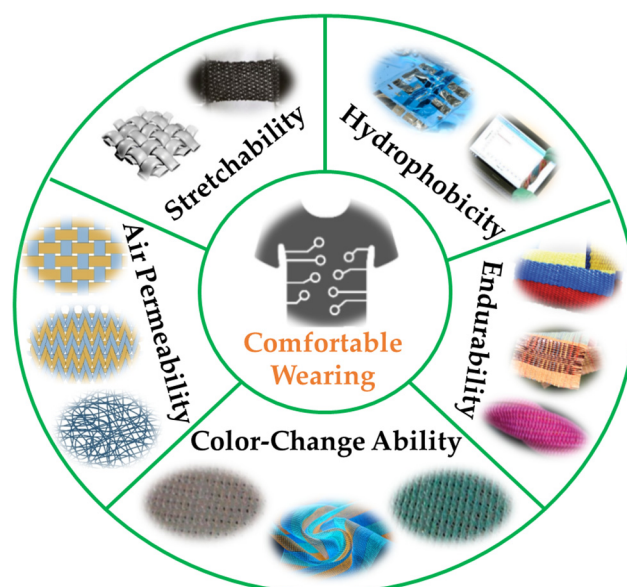


**Figure 18.** Characteristics required for fabric-type wearable devices for comfortable wearing.

For enhancing stretchability, numerous conducting materials such as carbon-based materials, conductive polymers, and metal-based nanostructures, have been integrated into elastomeric matrices, thereby facilitating the fabrication of highly stretchable electrodes. Additionally, various specific geometrical configurations, including an open-mesh structure, buckling structure, island–bridge structure, and serpentine pattern, have been introduced to enhance the overall stretchability of fabric-type wearable electronics. However, despite significant progress in this domain, there remain opportunities for further improvements in electrical conductivity and simplification of electrode structure design. These constraints pose challenges to device fabrication and integration, and have subsequently emerged as pivotal focal points for large-scale deployment and commercialization efforts.

For improving hydrophobic performance, various coating materials have been developed to coat on the surfaces of fibers or fabrics. Hydrophobic coating methods have served to further elevate the overall hydrophobic properties of textile-based devices. Through

integrating coating materials and coating methods, smart fabrics can maintain the flexibility and comfort of the fabric while achieving waterproof properties. Although smart fabrics have achieved good results in water resistance, there are still some challenges and limitations. Among these, the balance between waterproof performance and breathability is still a problem to be solved. Maximizing the breathability of the fabric while ensuring the waterproof effect is one of the keys to the future development of smart fabrics.

To verify stability, including mechanical and chemical stability, rigorous evaluation is necessary for all materials and fabrication processes used in the creation of fabric-type wearable electronics. Furthermore, the working stability under complicate environments must also be tested, which is essential to eliminate any potential risks before application in wearable applications. Notably, since the function of these fabrics depends on conductive materials, it is critical to ensure that their electrical properties remain consistent over time and across environments. This requires the development of more stable and reliable conductive materials and manufacturing techniques.

Researchers have made significant progress in improving air permeability, achieved through the development of various permeable materials and textile structure designs. These advances enable smart fabrics to maintain their functionality while allowing air and moisture to circulate freely, thereby increasing the wearer's comfort. However, there is still room for improvement in the breathability of smart fabrics. One aspect involves balancing air permeability with other desired properties such as water resistance and electrical conductivity. Another relates to the potential for the breathability of smart fabrics to be affected by factors such as fabric thickness, fiber density, and the presence of additional layers or coatings. Therefore, further research and development are needed to optimize these factors and enhance the breathability of smart fabrics.

To satisfy the requirements of multifunctional wearing experiences, significant progress has been made in the field of smart color-change fabrics, especially in terms of color-change materials. However, the fabrication of smart color-changing fabrics is difficult since the distance of electron transfer and ion diffusion increases with fiber length, resulting in an increase in color-change time, resulting in uniform color changes in smart color-changing fabric. Furthermore, another challenge is that current smart fabrics are often unable to achieve certain color variations. Therefore, by advancing the understanding of the mechanisms governing color change in fibers and developing innovative materials and processes, the way can be paved for the creation of smart fabrics that exhibit dynamic and responsive color characteristics.

In a word, the integration of multiple functions encompassing exceptional stretchability, hydrophobicity, stability, air permeability, and color-change ability into smart electronic textiles is expected to further the progress toward comfortable wearing and facilitate the wide-spread adoption of electronic textiles in the future.

**Author Contributions:** Conceptualization, H.X., C.L. and X.F.; investigation, H.X. and C.L.; writing—original draft preparation, H.X., Y.L., Q.L. and C.L.; writing—review and editing, H.X., L.X., H.Z. and X.W.; supervision, X.F. and C.L.; project administration, X.F.; funding acquisition, X.F. All authors have read and agreed to the published version of the manuscript.

**Funding:** We are grateful to the State Grid Chongqing Electric Power Research Institute for the Key Science and Technology project funding (Research and application of wearable outdoor Active cooling protective clothing).

**Data Availability Statement:** The data presented in this study are available in this article.

**Conflicts of Interest:** The authors declare no conflicts of interest.

## References

1. Gong, S.; Lu, Y.; Yin, J.; Levin, A.; Cheng, W. Materials-driven soft wearable bioelectronics for connected healthcare. *Chem. Rev.* **2024**, *124*, 455–553. [[CrossRef](#)] [[PubMed](#)]
2. Brasier, N.; Frobert, O.; De Ieso, F.; Meyer, D.; Kowatsch, T.; Ghaffari, R. The potential of wearable sweat sensors in heart failure management. *Nat. Electron.* **2024**, *7*, 182–184. [[CrossRef](#)]

3. Ye, C.; Wang, M.; Min, J.; Tay, R.Y.; Lukas, H.; Sempionatto, J.R.; Li, J.H.; Xu, C.H.; Gao, W. A wearable aptamer nanobiosensor for non-invasive female hormone monitoring. *Nat. Nanotechnol.* **2024**, *19*, 330–337. [[CrossRef](#)] [[PubMed](#)]
4. Ates, H.C.; Ates, C.; Dincer, C. Stress monitoring with wearable technology and AI. *Nat. Electron.* **2024**, *7*, 98–99. [[CrossRef](#)]
5. Che, Z.; Wan, X.; Xu, J.; Duan, C.; Zheng, T.Q.; Chen, J. Speaking without vocal folds using a machine-learning-assisted wearable sensing-actuation system. *Nat. Commun.* **2024**, *15*, 1873. [[CrossRef](#)] [[PubMed](#)]
6. Chen, G.R.; Xiao, X.; Zhao, X.; Tat, T.; Bick, M.; Chen, J. Electronic textiles for wearable point-of-care systems. *Chem. Rev.* **2022**, *122*, 3259–3291. [[CrossRef](#)] [[PubMed](#)]
7. Yao, K.; Zhou, J.; Huang, Q.; Wu, M.; Yiu, C.K.; Li, J.; Huang, X.; Li, D.; Su, J.; Hou, S.; et al. Encoding of tactile information in hand via skin-integrated wireless haptic interface. *Nat. Mach. Intell.* **2022**, *4*, 893–903. [[CrossRef](#)]
8. Wang, S.; Xu, J.; Wang, W.; Wang, G.-J.N.; Rastak, R.; Molina-Lopez, F.; Chung, J.W.; Niu, S.; Feig, V.R.; Lopez, J.; et al. Skin electronics from scalable fabrication of an intrinsically stretchable transistor array. *Nature* **2018**, *555*, 83–88. [[CrossRef](#)] [[PubMed](#)]
9. Huang, Q.Y.; Zheng, Z.J. Pathway to developing permeable electronics. *ACS Nano* **2022**, *16*, 15537–15544. [[CrossRef](#)] [[PubMed](#)]
10. Luo, Y.; Abidian, M.R.; Ahn, J.-H.; Akinwande, D.; Andrews, A.M.; Antonietti, M.; Bao, Z.; Berggren, M.; Berkey, C.A.; Bettinger, C.J.; et al. Technology roadmap for flexible sensors. *ACS Nano* **2023**, *17*, 5211–5295. [[CrossRef](#)] [[PubMed](#)]
11. Kim, J.; Campbell, A.S.; de Avila, B.E.; Wang, J. Wearable biosensors for healthcare monitoring. *Nat. Biotechnol.* **2019**, *37*, 389–406. [[CrossRef](#)] [[PubMed](#)]
12. Hou, B.; Yi, L.; Li, C.; Zhao, H.; Zhang, R.; Zhou, B.; Liu, X. An interactive mouthguard based on mechanoluminescence-powered optical fibre sensors for bite-controlled device operation. *Nat. Electron.* **2022**, *5*, 682–693. [[CrossRef](#)]
13. Li, J.; Carlos, C.; Zhou, H.; Sui, J.; Wang, Y.; Silva-Pedraza, Z.; Yang, F.; Dong, Y.; Zhang, Z.; Hacker, T.A.; et al. Stretchable piezoelectric biocrystal thin films. *Nature Commun.* **2023**, *14*, 6562. [[CrossRef](#)] [[PubMed](#)]
14. Khanh, T.D.; Meena, J.S.; Choi, S.B.; Kim, J.W. Breathable, self-healable, washable and durable all-fibrous triboelectric nanogenerator for wearable electronics. *Mater. Today Adv.* **2023**, *20*, 100427. [[CrossRef](#)]
15. Song, E.; Li, J.; Won, S.M.; Bai, W.; Rogers, J.A. Materials for flexible bioelectronic systems as chronic neural interfaces. *Nat. Mater.* **2020**, *19*, 590–603. [[CrossRef](#)]
16. Feng, T.; Ling, D.; Li, C.; Zheng, W.; Zhang, S.; Li, C.; Emel'yanov, A.; Pozdnyakov, A.S.; Lu, L.; Mao, Y. Stretchable on-skin touchless screen sensor enabled by ionic hydrogel. *Nano Res.* **2024**, *17*, 4462–4470. [[CrossRef](#)]
17. Shen, Q.; Jiang, M.; Wang, R.; Song, K.; Vong, M.H.; Jung, W.; Krisnadi, F.; Kan, R.; Zheng, F.; Fu, B.; et al. Liquid Metal-based soft, hermetic, and wireless-communicable seals for stretchable systems. *Science* **2023**, *379*, 488–493. [[CrossRef](#)]
18. Xie, C.; Chang, J.; Shang, J.; Wang, L.; Gao, Y.; Huang, Q.; Zheng, Z. Hybrid lithium-ion/metal electrodes enable long cycle stability and high energy density of flexible batteries. *Adv. Funct. Mater.* **2022**, *32*, 2203242. [[CrossRef](#)]
19. Lu, Y.; Sathasivam, S.; Song, J.; Crick, C.R.; Carmalt, C.J.; Parkin, I.P. Robust self-cleaning surfaces that function when exposed to either air or oil. *Science* **2015**, *347*, 1132–1135. [[CrossRef](#)] [[PubMed](#)]
20. Zhang, W.; Wang, D.; Sun, Z.; Song, J.; Deng, X. Robust superhydrophobicity: Mechanisms and strategies. *Chem. Soc. Rev.* **2021**, *50*, 4031. [[CrossRef](#)] [[PubMed](#)]
21. Wang, D.; Sun, Q.; Hokkanen, M.J.; Zhang, C.; Lin, F.-Y.; Liu, Q.; Zhu, S.-P.; Zhou, T.; Chang, Q.; He, B. Design of robust superhydrophobic surfaces. *Nature* **2020**, *582*, 55–59. [[CrossRef](#)] [[PubMed](#)]
22. Celik, N.; Torun, I.; Ruzi, M.; Esidir, A.; Onses, M.S. Fabrication of robust superhydrophobic surfaces by one-step spray coating: Evaporation driven self-assembly of wax and nanoparticles into hierarchical structures. *Chem. Eng. J.* **2020**, *396*, 12523. [[CrossRef](#)]
23. Ma, Z.; Huang, Q.; Xu, Q.; Zhuang, Q.; Zhao, X.; Yang, Y.; Qiu, H.; Yang, Z.; Wang, C.; Chai, Y.; et al. Permeable superelastic liquid-metal fibre mat enables biocompatible and monolithic stretchable electronics. *Nat. Mater.* **2021**, *20*, 859–868. [[CrossRef](#)] [[PubMed](#)]
24. Zheng, Z.; Jur, J.; Cheng, W. Smart materials and devices for electronic textiles. *MRS Bull.* **2021**, *46*, 488–490. [[CrossRef](#)]
25. Chen, M.; Li, P.; Wang, R.; Xiang, Y.; Huang, Z.; Yu, Q.; He, M.; Liu, J.; Wang, J.; Su, M.; et al. Multifunctional fiber-enabled intelligent health agents. *Adv. Mater.* **2022**, *34*, 2200985. [[CrossRef](#)] [[PubMed](#)]
26. Kaltenbrunner, M.; Sekitani, T.; Reeder, J.; Yokota, T.; Kuribara, K.; Tokuhara, T.; Drack, M.; Schwödiauer, R.; Graz, I.; Bauer-Gogonea, S.; et al. An ultra-lightweight design for imperceptible plastic electronics. *Nature* **2013**, *499*, 458–463. [[CrossRef](#)] [[PubMed](#)]
27. Miyamoto, A.; Lee, S.; Cooray, N.F.; Lee, S.; Mori, M.; Matsuhisa, N.; Jin, H.; Yoda, L.; Yokota, T.; Itoh, A.; et al. Inflammation-free, gas-permeable, lightweight, stretchable on-skin electronics with nanomeshes. *Nat. Nanotechnol.* **2017**, *12*, 907. [[CrossRef](#)] [[PubMed](#)]
28. Lim, H.; Kim, H.; Qazi, R.; Kwon, Y.; Jeong, J.; Yeo, W. Advanced soft materials, sensor integrations, and applications of wearable flexible hybrid electronics in healthcare, energy, and environment. *Adv. Mater.* **2020**, *32*, 1901924. [[CrossRef](#)] [[PubMed](#)]
29. Wang, Y.; Lee, S.; Wang, H.; Jiang, Z.; Jimbo, Y.; Wang, C.; Wang, B.; Kim, J.J.; Koizumi, M.; Yokota, T.; et al. Robust, self-adhesive, reinforced polymeric nanofilms enabling gas-permeable dry electrodes for long-term application. *Proc. Natl. Acad. Sci. USA* **2021**, *118*, e2111904118. [[CrossRef](#)] [[PubMed](#)]
30. Choi, C.; Lee, J.M.; Kim, S.H.; Kim, S.J.; Di, J.; Baughman, R.H. Twistable and stretchable sandwich structured fiber for wearable sensors and supercapacitors. *Nano Lett.* **2016**, *16*, 7677–7684. [[CrossRef](#)] [[PubMed](#)]
31. Gu, C.; Jia, A.-B.; Zhang, Y.-M.; Zhang, S.X.-A. Emerging electrochromic materials and devices for future displays. *Chem. Rev.* **2022**, *122*, 14679–14721. [[CrossRef](#)] [[PubMed](#)]

32. Chou, H.-H.; Nguyen, A.; Chortos, A.; To, J.W.F.; Lu, C.; Mei, J.; Kurosawa, T.; Bae, W.-G.; Tok, J.B.-H.; Bao, Z. A chameleon-inspired stretchable electronic skin with interactive colour changing controlled by tactile sensing. *Nat. Commun.* **2015**, *6*, 8011. [[CrossRef](#)] [[PubMed](#)]
33. Sheng, M.; Li, J.; Jiang, X.; Wang, C.; Li, J.; Zhang, L.; Fu, S. Biomimetic solid–liquid transition structural dye-doped liquid crystal/phase-change-material microcapsules designed for wearable bistable electrochromic fabric. *ACS Appl. Mater. Interfaces* **2021**, *13*, 33282–33290. [[CrossRef](#)] [[PubMed](#)]
34. Ding, Y.; Invernale, M.A.; Sotzing, G.A. Conductivity trends of PEDOT-PSS impregnated fabric and the effect of conductivity on electrochromic textile. *ACS Appl. Mater. Interfaces* **2010**, *2*, 1588–1593. [[CrossRef](#)] [[PubMed](#)]
35. Zhang, Y.; Hu, Z.; Xiang, H.; Zhai, G.; Zhu, M. Fabrication of visual textile temperature indicators based on reversible thermochromic fibers. *Dyes Pigm.* **2019**, *162*, 705–711. [[CrossRef](#)]
36. Wang, C.; Jiang, X.; Cui, P.; Sheng, M.; Gong, X.; Zhang, L.; Fu, S. Multicolor and multistage response electrochromic color-memory wearable smart textile and flexible display. *ACS Appl. Mater. Interfaces* **2021**, *13*, 12313–12321. [[CrossRef](#)]
37. Sekitani, T.; Noguchi, Y.; Hata, K.; Fukushima, T.; Aida, T.; Someya, T. A Rubberlike stretchable active matrix using elastic conductors. *Science* **2008**, *321*, 1468–1472. [[CrossRef](#)] [[PubMed](#)]
38. Zhang, Z.; Wang, W.; Jiang, Y.; Wang, Y.; Wu, Y.; Lai, J.; Niu, S.; Xu, C.; Shih, C.; Wang, C.; et al. High-brightness all-polymer stretchable LED with charge-trapping dilution. *Nature* **2022**, *603*, 624–630. [[CrossRef](#)]
39. Guan, Y.S.; Zhang, Z.; Tang, Y.; Yin, J.; Ren, S. Kirigami-inspired nanoconfined polymer conducting nanosheets with 2000% stretchability. *Adv. Mater.* **2018**, *30*, 1706390. [[CrossRef](#)] [[PubMed](#)]
40. Xu, J.; Wang, S.; Wang, G.; Zhu, C.; Luo, S.; Jin, L.; Gu, X.; Chen, S.; Feig, V.; To, J.; et al. Highly stretchable polymer semiconductor films through the nanoconfinement effect. *Science* **2017**, *355*, aah4496. [[CrossRef](#)] [[PubMed](#)]
41. Zhao, Y.; Zhang, B.; Yao, B.; Qiu, Y.; Peng, Z.; Zhang, Y.; Alsaied, Y.; Frenkel, I.; Youssef, K.; Pei, Q.; et al. Hierarchically structured stretchable conductive hydrogels for high-performance wearable strain sensors and supercapacitors. *Matter* **2020**, *3*, 1196–1210. [[CrossRef](#)]
42. Shao, B.; Lu, M.; Wu, T.; Peng, W.; Ko, T.; Hsiao, Y.; Chen, J.; Sun, B.; Liu, R.; Lai, Y. Large-area, untethered, metamorphic, and omnidirectionally stretchable multiplexing self-powered triboelectric skins. *Nat. Commun.* **2024**, *15*, 1238. [[CrossRef](#)]
43. Zhu, Y.; Xu, F. Buckling of aligned carbon nanotubes as stretchable conductors: A new manufacturing strategy. *Adv. Mater.* **2012**, *24*, 1073–1077. [[CrossRef](#)] [[PubMed](#)]
44. Song, B.; He, W.; Wang, X.; Zeng, X.; Cheng, M.; Wu, F.; Moon, K.; Wong, C. Fabrication of stretchable and conductive polymer nanocomposites based on interconnected graphene aerogel. *Compos. Sci. Technol.* **2020**, *200*, 108430. [[CrossRef](#)]
45. Lim, T.; Kim, H.; Won, S.; Kim, C.; Yoo, J.; Lee, J.; Son, K.; Nam, I.; Kim, K.; Yeo, S.; et al. Liquid metal-based electronic textiles coated with Au nanoparticles as stretchable electrode materials for healthcare monitoring. *ACS Appl. Nano Mater.* **2023**, *6*, 8482–8494. [[CrossRef](#)]
46. Zhu, B.; Gong, S.; Lin, F.; Wang, Y.; Ling, Y.Z.; An, T.; Cheng, W. Patterning vertically grown gold nanowire electrodes for intrinsically stretchable organic transistors. *Adv. Electron. Mater.* **2018**, *5*, 1800509. [[CrossRef](#)]
47. Hirsch, A.; Michaud, H.O.; Gerratt, A.P.; Mulatier, S.; Lacour, S. Intrinsically stretchable biphasic (solid–liquid) thin metal films. *Adv. Mater.* **2016**, *28*, 4507–4512. [[CrossRef](#)] [[PubMed](#)]
48. Zhu, P.; Mu, S.; Huang, W.; Sun, Z.; Lin, Y.; Chen, K.; Pan, Z.; Haghighi, M.G.; Sedghi, R.; Wang, J.; et al. Soft multifunctional neurological electronic skin through intrinsically stretchable synaptic transistor. *Nano Res.* **2024**. [[CrossRef](#)]
49. Guo, X.; Facchetti, A. The journey of conducting polymers from discovery to application. *Nat. Mater.* **2020**, *19*, 922–928. [[CrossRef](#)]
50. Tang, H.; Liang, Y.; Liu, C.; Hu, Z.; Deng, Y.; Guo, H.; Yu, Z.; Song, A.; Zhao, H.; Zhao, D.; et al. A solution-processed n-type conducting polymer with ultrahigh conductivity. *Nature* **2022**, *611*, 271. [[CrossRef](#)] [[PubMed](#)]
51. Mokhtar, S.M.A.; Alvarez de Eulate, E.; Yamada, M.; Prow, T.W.; Evans, D.R. Conducting polymers in wearable devices. *Med. Devices Sens.* **2021**, *4*, e10160. [[CrossRef](#)]
52. Bao, Z.; Chen, X. Flexible and stretchable devices. *Adv. Mater.* **2016**, *28*, 4177–4179. [[CrossRef](#)] [[PubMed](#)]
53. Bandodkar, A.J.; Jeerapan, I.; You, J.-M.; Nuñez-Flores, R.; Wang, J. Highly stretchable fully-printed CNT-based electrochemical sensors and biofuel cells: Combining intrinsic and design-induced stretchability. *Nano Lett.* **2016**, *16*, 721–727. [[CrossRef](#)] [[PubMed](#)]
54. Chen, W.; Xiao, H.; Zhou, X.; Xu, X.; Jiang, S.; Qin, Z.; Ding, S.; Bian, C.; Liu, Z. Highly deformable graphene/poly(3,4-ethylenedioxythiophene): Poly(styrene Sulfonate) hydrogel composite film for stretchable supercapacitors. *ACS Appl. Energy Mater.* **2022**, *5*, 7277–7286. [[CrossRef](#)]
55. Zhang, Y.; Guo, X.; Huang, J.; Ren, Z.; Hu, H.; Li, P.; Lu, X.; Wu, Z.; Xiao, T.; Zhu, Y.; et al. Solution process formation of high performance, stable nanostructured transparent metal electrodes via displacement-diffusion-etch process. *NPJ Flex. Electron.* **2022**, *6*, 4. [[CrossRef](#)]
56. Oh, S.Y.; Hong, S.; Jeong, Y.; Yun, J.; Park, H.; Jin, S.; Lee, G.; Oh, J.; Lee, H.; Lee, S.; et al. Skin-attachable, stretchable electrochemical sweat sensor for glucose and pH detection. *ACS Appl. Mater. Interfaces* **2018**, *10*, 13729–13740. [[CrossRef](#)] [[PubMed](#)]
57. Gong, S.; Schwalb, W.; Wang, Y.; Chen, Y.; Tang, J.; Shirinzadeh, S.B.; Cheng, W. A wearable and highly sensitive pressure sensor with ultrathin gold nanowires. *Nat. Commun.* **2014**, *5*, 3132. [[CrossRef](#)]



58. Ding, S.; Jiang, Z.; Chen, F.; Fu, L.; Lv, Y.; Qian, Y.; Zhao, S. Intrinsically stretchable, transient conductors from a composite material of Ag flakes and gelatin hydrogel. *ACS Appl. Mater. Interfaces* **2020**, *12*, 27572–27577. [[CrossRef](#)] [[PubMed](#)]
59. Ma, J.; Wang, P.; Chen, H.; Bao, S.; Chen, W.; Lu, H. Highly sensitive and large-range strain sensor with a self-compensated two-order structure for human motion detection. *ACS Appl. Mater. Interfaces* **2019**, *11*, 8527–8536. [[CrossRef](#)] [[PubMed](#)]
60. Son, W.; Chun, S.; Lee, J.; Lee, Y.; Park, J.; Suh, D.; Lee, D.; Jung, H.; Kim, Y.; Kim, Y.; et al. Highly twisted supercoils for superelastic multifunctional fibres. *Nat. Commun.* **2019**, *10*, 426. [[CrossRef](#)] [[PubMed](#)]
61. Lee, H.B.; Bae, C.W.; Duy, L.T.; Sohn, I.Y.; Kim, D.I.; Song, Y.J.; Kim, Y.J.; Lee, N.E. Mogul-patterned elastomeric substrate for stretchable electronics. *Adv. Mater.* **2016**, *28*, 3069–3077. [[CrossRef](#)] [[PubMed](#)]
62. Kim, S.H.; Jung, S.; Yoon, I.S.; Lee, C.; Oh, Y.; Hong, J.M. Ultrastretchable conductor fabricated on skin-like hydrogel-elastomer hybrid substrates for skin electronics. *Adv. Mater.* **2018**, *30*, 1800109. [[CrossRef](#)] [[PubMed](#)]
63. Hua, Q.; Shen, G. Low-dimensional nanostructures for monolithic 3D-integrated flexible and stretchable electronics. *Chem. Soc. Rev.* **2024**, *53*, 1316. [[CrossRef](#)] [[PubMed](#)]
64. Kwak, J.; Jeong, J.; Kwon, Y.; Seo, D.; Kang, C.; Kim, D.; Han, J.; Gwak, E.; Choi, D.; Kim, J.; et al. Manufacturing of stretchable substrate with biaxial strain control for highly-efficient stretchable solar cells and displays. *Sci. Rep.* **2023**, *13*, 20460. [[CrossRef](#)]
65. Bian, Y.; Zhu, M.; Wang, C.; Liu, K.; Shi, W.; Zhu, Z.; Qin, M.; Zhang, F.; Zhao, Z.; Wang, H.; et al. A detachable interface for stable low-voltage stretchable transistor arrays and high-resolution X-ray imaging. *Nat. Commun.* **2024**, *15*, 2624. [[CrossRef](#)]
66. Narayana, H.; Le, K.; Nakayama, C.; Yang, C.; Wang, Z.; Eng, J.J.; Servati, P. Capturing complex hand movements and object interactions using machine learning-powered stretchable smart textile gloves. *Nat. Mach. Intell.* **2024**, *6*, 106–118.
67. Kim, K.; Park, S.; Park, S.; Kim, I.; Park, B.; Kim, S.; Jeong, U.; Kim, J.; Yang, C. Deformable micro-supercapacitor fabricated via laser ablation patterning of graphene/liquid metal. *npj Flex. Electron.* **2024**, *8*, 18. [[CrossRef](#)]
68. Park, H.; Kim, J.; Hong, S.; Lee, G.; Lee, H.; Song, C.; Keum, K.; Jeong, Y.; Jin, S.; Kim, D.; et al. Dynamically stretchable supercapacitor for powering an integrated biosensor in an all-in-one textile system. *ACS Nano* **2019**, *13*, 10469–10480. [[CrossRef](#)] [[PubMed](#)]
69. Kwon, H.; Kim, G.; Lim, C.; Kim, J.; Lee, S.; Cho, J.; Koo, H.; Kim, B.; Char, K.; Son, J. Sequentially Coated Wavy Nanowire Composite Transparent Electrode for Stretchable Solar Cells. *ACS Appl. Mater. Interfaces* **2023**, *15*, 13656–13667. [[CrossRef](#)] [[PubMed](#)]
70. Huang, F.; Yu, H.; Xiang, S.; Xue, J.; Ming, H.; Tao, C.; Zhang, N.; Fan, X. Embroidering a filmsy photo rechargeable energy fabric with wide weather adaptability. *ACS Appl. Mater. Interfaces* **2020**, *12*, 3654–3660. [[CrossRef](#)] [[PubMed](#)]
71. Song, Y.; Nguyen, T.; Lee, D.; Kim, J. Machine learning-enabled environmentally adaptable skin-electronic sensor for human gesture recognition. *ACS Appl. Mater. Interfaces* **2024**, *16*, 9551–9560. [[CrossRef](#)] [[PubMed](#)]
72. Yang, C.; Wang, Y.; Wang, Y.; Zhao, Z.; Zhang, L.; Chen, H. Highly stretchable PTFE particle enhanced triboelectric nanogenerator for droplet energy harvestings. *Nano Energy* **2023**, *118*, 109000. [[CrossRef](#)]
73. Jiang, J.; Shen, Y.; Xu, Y.; Wang, Z.; Tao, J.; Liu, S.; Liu, W.; Chen, H. An energy-free strategy to elevate anti-icing performance of superhydrophobic materials through interfacial airflow manipulation. *Nat. Commun.* **2024**, *15*, 777. [[CrossRef](#)] [[PubMed](#)]
74. Ma, W.; Yang, Z.; Asif, M.; Zhang, Y.; Li, W.; Yang, J.; Yao, S. Scalable-manufactured anticorrosion and wear-resistant superhydrophobic surfaces. *ACS Appl. Eng. Mater.* **2023**, *1*, 519–529. [[CrossRef](#)]
75. Zhao, Z.; Zhang, Q.; Song, X.; Chen, J.; Ding, Y.; Wu, H.; Guo, S. Versatile melanin-like coatings with hierarchical structure toward personal thermal management, anti-icing/deicing, and UV protection. *ACS Appl. Mater. Interfaces* **2023**, *15*, 3522–3533. [[CrossRef](#)] [[PubMed](#)]
76. Tian, T.; Yang, M.; Fang, Y.; Zhang, S.; Chen, Y.; Wang, L.; Wu, W. Large-area waterproof and durable perovskite luminescent textiles. *Nat. Commun.* **2023**, *14*, 234. [[CrossRef](#)] [[PubMed](#)]
77. Ding, Y.; Liu, R.; Zheng, Y.; Wang, X.; Yu, Y. Fabrication of a superhydrophobic conductive porous film with water-resistance for wearable sensors. *ACS Appl. Electron. Mater.* **2023**, *5*, 440–450. [[CrossRef](#)]
78. Qahtan, T.F.; Gondal, M.A.; Alade, I.O.; Dastageer, M.A. Fabrication of water jet resistant and thermally stable superhydrophobic surfaces by spray coating of candle soot dispersion. *Sci. Rep.* **2017**, *7*, 7531. [[CrossRef](#)] [[PubMed](#)]
79. Wang, Z.; Zhang, X.; Cao, T.; Wang, T.; Sun, L.; Wang, K.; Fan, X. Antiliquid-Interfering, antibacteria, and adhesive wearable strain sensor based on superhydrophobic and conductive composite hydrogel. *ACS Appl. Mater. Interfaces* **2021**, *13*, 46022–46032. [[CrossRef](#)] [[PubMed](#)]
80. Chen, X.; Wang, M.; Xin, Y.; Huang, Y. One-step fabrication of self-cleaning superhydrophobic surfaces: A combined experimental and molecular dynamics study. *Surf. Interfaces* **2022**, *31*, 102022. [[CrossRef](#)]
81. Barthwal, S.; Lee, B.; Lim, S.H. Fabrication of robust and durable slippery anti-icing coating on textured superhydrophobic aluminum surfaces with infused silicone oil. *Appl. Surf. Sci.* **2019**, *496*, 143677. [[CrossRef](#)]
82. Zhu, B.; Ou, R.; Liu, J.; Yang, Y.; Chen, S.; Wei, G.; Zhang, Z. Fabrication of superhydrophobic surfaces with hierarchical structure and their corrosion resistance and self-cleaning properties. *Surf. Interfaces* **2022**, *28*, 101608.
83. He, Q.; Wang, J.; Wang, G.; Hao, X.; Li, A. Construction of a durable superhydrophobic flame-retardant coating on the PET fabrics. *Mater. Des.* **2023**, *233*, 112258. [[CrossRef](#)]
84. Zhu, X.; Zhang, Z.; Ge, B.; Men, X.; Zhou, X. Fabrication of a superhydrophobic carbon nanotube coating with good reusability and easy repairability. *Colloids Surf. A* **2014**, *444*, 252–256. [[CrossRef](#)]

85. Peng, S.; Tian, D.; Yang, X.; Deng, W. Highly efficient and large-scale fabrication of superhydrophobic alumina surface with strong stability based on self-congregated alumina nanowires. *ACS Appl. Mater. Interfaces* **2014**, *6*, 4831–4841. [[CrossRef](#)] [[PubMed](#)]
86. He, B.; Hou, X.; Liu, Y.; Hu, J.; Song, L.; Tong, Z.; Zhan, X.; Ren, Y.; Liu, Q.; Zhang, Q. Design of fluorine-free waterborne fabric coating with robust hydrophobicity, water-resistant and breathability. *Sep. Purif. Technol.* **2023**, *311*, 123308. [[CrossRef](#)]
87. Wang, M.; Zhang, M.; Pang, L.; Yang, C.; Zhang, Y.; Hu, J.; Wu, G. Fabrication of highly durable polysiloxane-zinc oxide (ZnO) coated polyethylene terephthalate (PET) fabric with improved ultraviolet resistance, hydrophobicity, and thermal resistance. *J. Colloid Interface Sci.* **2019**, *537*, 91–100. [[CrossRef](#)] [[PubMed](#)]
88. Dominic, J.; Perumal, G.; Grewal, H.S.; Arora, H.S. Facile fabrication of superhydrophobic brass surface for excellent corrosion resistance. *Surf. Eng.* **2020**, *36*, 660–664. [[CrossRef](#)]
89. Wang, J.; Chen, Y. Oil–water separation capability of superhydrophobic fabrics fabricated via combining polydopamine adhesion with lotus-leaf-like structure. *J. Appl. Polym. Sci.* **2015**, *132*, 42614. [[CrossRef](#)]
90. Xue, C.; Fan, Q.; Guo, X.; An, Q.; Jia, S. Fabrication of superhydrophobic cotton fabrics by grafting of POSS-based polymers on fibers. *Appl. Surf. Sci.* **2019**, *465*, 241–248. [[CrossRef](#)]
91. Leng, B.; Shao, Z.; With, G.; Ming, W. Superoleophobic cotton textiles. *Langmuir* **2009**, *25*, 2456–2460. [[CrossRef](#)] [[PubMed](#)]
92. Tang, Y.; Sun, K.; Du, X.; Zhao, J.; Wang, H.; Huang, Q. Superhydrophobic electrospun FPI/PTFE nanofiber membranes for robust vacuum membrane distillation. *Sep. Purif. Technol.* **2023**, *326*, 124856. [[CrossRef](#)]
93. Xue, C.; Jia, S.; Zhang, J.; Tian, L. Superhydrophobic surfaces on cotton textiles by complex coating of silica nanoparticles and hydrophobization. *Thin Solid Film.* **2009**, *517*, 4593–4598. [[CrossRef](#)]
94. Ye, Y.; Kang, Z.; Wang, F.; Long, Y.; Guo, T.; Chen, D.; Kong, J.; Xu, L. Achieving hierarchical structure with superhydrophobicity and enhanced anti-corrosion via electrochemical etching and chemical vapor deposition. *Appl. Surf. Sci.* **2023**, *610*, 155362. [[CrossRef](#)]
95. Liao, X.; Li, H.; Zhang, L.; Su, X.; Lai, X.; Zeng, X. Superhydrophobic MGO/PDMS hybrid coating on polyester fabric for oil/water separation. *Prog. Org. Coat.* **2018**, *115*, 172–180. [[CrossRef](#)]
96. Chen, J.; Yuan, L.; Shi, C.; Wu, C.; Long, Z.; Qiao, H.; Wang, K.; Fan, Q.H. Nature-inspired hierarchical protrusion structure construction for washable and wear-resistant superhydrophobic textiles with self-cleaning ability. *ACS Appl. Mater. Interfaces* **2021**, *13*, 18142–18151. [[CrossRef](#)] [[PubMed](#)]
97. Abu-Thabit, N.Y.; Azad, A.K.; Mezghani, K.; Hakeem, A.S.; Drmash, Q.A.; Akhtar, S.; Adesina, A.Y. Facile and green fabrication of superhydrophobic polyacrylonitrile nonwoven fabric with iron hydroxide nanoparticles for efficient oil/water separation. *ACS Appl. Polym. Mater.* **2022**, *4*, 8450–8460. [[CrossRef](#)]
98. Chen, X.; He, Y.; Tian, M.; Qu, L.; Fan, T.; Miao, J. Core–sheath heterogeneous interlocked conductive fiber enables smart textile for personalized healthcare and thermal management. *Small* **2023**, *19*, 2308404. [[CrossRef](#)] [[PubMed](#)]
99. Yang, Y.; Zhang, N.; Zhang, B.; Zhang, Y.; Tao, C.; Wang, J.; Fan, X. Highly-efficient dendritic cable electrodes for flexible supercapacitive fabric. *ACS Appl. Mater. Interfaces* **2017**, *9*, 40207–40214. [[CrossRef](#)] [[PubMed](#)]
100. Xiong, S.; Fukuda, K.; Nakano, K.; Lee, S.; Sumi, Y.; Takakuwa, M.; Inoue, D.; Hashizume, D.; Du, B.; Yokota, T.; et al. Waterproof and ultraflexible organic photovoltaics with improved interface adhesion. *Nat. Commun.* **2024**, *15*, 681. [[CrossRef](#)] [[PubMed](#)]
101. Zhang, N.; Chen, J.; Huang, Y.; Guo, W.; Yang, J.; Du, J.; Fan, X.; Tao, C. A wearable all-solid photovoltaic textile. *Adv. Mater.* **2016**, *28*, 263–269. [[CrossRef](#)] [[PubMed](#)]
102. Zhu, T.; Ni, Y.; Zhao, K.; Huang, J.; Cheng, Y.; Ge, M.; Park, C.; Lai, Y. A breathable knitted fabric-based smart system with enhanced superhydrophobicity for drowning alarming. *ACS Nano* **2022**, *16*, 18018–18026. [[CrossRef](#)] [[PubMed](#)]
103. Kang, M.H.; Lee, G.J.; Lee, J.H.; Kim, M.S.; Yan, Z.; Jeong, J.-W.; Jang, K.-I.; Song, Y.M. Outdoor-useable, wireless/battery-free patch-type tissue oximeter with radiative cooling. *Adv. Sci.* **2021**, *8*, 2004885. [[CrossRef](#)] [[PubMed](#)]
104. Zhang, J.-H.; Li, Z.; Xu, J.; Li, J.; Yan, K.; Cheng, W.; Xin, M.; Zhu, T.; Du, J.; Chen, S.; et al. Versatile self-assembled electrospun micropylam arrays for high-performance on-skin devices with minimal sensory interference. *Nat. Commun.* **2022**, *13*, 5839. [[CrossRef](#)] [[PubMed](#)]
105. Min, J.; Tu, J.; Xu, C.; Lukas, H.; Shin, S.; Yang, Y.; Solomon, S.A.; Mukasa, D.; Gao, W. Skin-interfaced wearable sweat sensors for precision medicine. *Chem. Rev.* **2023**, *123*, 5049–5138. [[CrossRef](#)] [[PubMed](#)]
106. Heo, J.H.; Sung, M.; Trung, T.Q.; Lee, Y.; Jung, D.H.; Kim, H.; Kaushal, S.; Lee, N.-E.; Kim, J.W.; Lee, J.H.; et al. Sensor design strategy for environmental and biological monitoring. *EcoMat* **2023**, *5*, e12332. [[CrossRef](#)]
107. Chen, F.; Huang, Q.; Zheng, Z. Permeable conductors for wearable and on-skin electronics. *Small Struct.* **2022**, *3*, 2100135. [[CrossRef](#)]
108. Zhang, J.; Wang, G.; Cui, J.; Tian, L.; Huang, Y. Breathability test for textiles. *Print. Dye* **2009**, *35*, 38–40.
109. Someya, T.; Amagai, M. Toward a new generation of smart skins. *Nat. Biotechnol.* **2019**, *37*, 382–388. [[CrossRef](#)] [[PubMed](#)]
110. Liu, S.; Rao, Y.; Jang, H.; Tan, P.; Lu, N. Strategies for body-conformable electronics. *Matter* **2022**, *5*, 1104–1136. [[CrossRef](#)]
111. Ding, Y.; Jiang, J.; Wu, Y.; Zhang, Y.; Zhou, J.; Zhang, Y.; Huang, Q.; Zheng, Z. Porous conductive textiles for wearable electronics. *Chem. Rev.* **2024**, *124*, 1535–1648. [[CrossRef](#)] [[PubMed](#)]
112. Xu, R.; Wu, G.; Jiang, M.; Cao, S.; Panahi-Sarmad, M.; Kamkar, M.; Xiao, X. Multi-stimuli dually-responsive intelligent woven structures with local programmability for biomimetic applications. *Small* **2023**, *19*, 2207900. [[CrossRef](#)] [[PubMed](#)]

113. Cao, R.; Pu, X.; Du, X.; Yang, W.; Wang, J.; Guo, H.; Zhao, S.; Yuan, Z.; Zhang, C.; Li, C.; et al. Screen-printed washable electronic textiles as self-powered touch/gesture tribo-sensor for intelligent human-machine interaction. *ACS Nano* **2018**, *12*, 5190–5196. [[CrossRef](#)]
114. Liang, X.; Zhu, M.; Li, H.; Dou, J.; Jian, M.; Xia, K.; Li, S.; Zhang, Y. Hydrophilic, breathable, and washable graphene decorated textile assisted by silk sericin for integrated multimodal smart wearables. *Adv. Funct. Mater.* **2022**, *32*, 2200162. [[CrossRef](#)]
115. Liu, H.; Zhou, F.; Shi, X.; Sun, K.; Kou, Y.; Das, P.; Li, Y.; Zhang, X.; Mateti, S.; Chen, Y.; et al. A thermoregulatory flexible phase change nonwoven for all season high efficiency wearable thermal management. *Nano-Micro Lett.* **2023**, *15*, 29. [[CrossRef](#)] [[PubMed](#)]
116. Tian, B.; Fang, Y.; Liang, J.; Zheng, K.; Guo, P.; Zhang, X.; Wu, Y.; Liu, Q.; Huang, Z.; Cao, C.; et al. Fully printed stretchable and multifunctional E-textiles for aesthetic wearable electronic systems. *Small* **2022**, *18*, 2107298. [[CrossRef](#)]
117. Zhou, W.; Yao, S.; Wang, H.; Du, Q.; Ma, Y.; Zhu, Y. Gas-permeable, ultrathin, stretchable epidermal electronics with porous electrodes. *ACS Nano* **2020**, *14*, 5798–5805. [[CrossRef](#)] [[PubMed](#)]
118. Chen, G.; Zhao, X.; Andalib, S.; Xu, J.; Zhou, Y.; Tat, T.; Lin, K.; Chen, J. Discovering giant magnetoelasticity in soft matter for electronic textiles. *Matter* **2021**, *4*, 3725–3740. [[CrossRef](#)] [[PubMed](#)]
119. Wang, P.; Ma, X.; Lin, Z.; Chen, F.; Chen, Z.; Hu, H.; Xu, H.; Zhang, X.; Shi, Y.; Huang, Q.; et al. Well-defined in-textile photolithography towards permeable textile electronics. *Nat. Commun.* **2024**, *15*, 887. [[CrossRef](#)] [[PubMed](#)]
120. Zhang, Y.; Wang, Y.; Wang, L.; Lo, C.; Zhao, Y.; Jiao, Y.; Zheng, G.; Peng, H. A fiber-shaped aqueous lithium-ion battery with high power density. *J. Mater. Chem. A* **2016**, *4*, 9002–9008. [[CrossRef](#)]
121. Li, Z.; Liu, Z.; Xu, S.; Zhang, K.; Zhao, D.; Pi, Y.; Guan, X.; Peng, Z.; Zhong, Q.; Zhong, J. Electrostatic smart textiles for braille-to-speech translation. *Adv. Mater.* **2024**, *36*, 2313518. [[CrossRef](#)] [[PubMed](#)]
122. Zhang, N.; Huang, F.; Zhao, S.; Lv, X.; Zhou, Y.; Xiang, S.; Xu, S.; Li, Y.; Chen, G.; Tao, C.; et al. Photo-rechargeable fabrics as sustainable and robust power sources for wearable bioelectronics. *Matter* **2020**, *2*, 1260–1269. [[CrossRef](#)]
123. Shin, M.; Song, J.H.; Lim, G.H.; Lim, B.; Park, J.J.; Jeong, U. Highly stretchable polymer transistors consisting entirely of stretchable device components. *Adv. Mater.* **2014**, *26*, 3706–3711. [[CrossRef](#)] [[PubMed](#)]
124. Chai, Z.; Zhang, N.; Sun, P.; Huang, Y.; Zhao, C.; Fan, H.; Fan, X.; Mai, W. Tailorable and wearable textile devices for solar energy harvesting and simultaneous storage. *ACS Nano* **2016**, *10*, 9201–9207. [[CrossRef](#)] [[PubMed](#)]
125. Liu, F.; Xu, S.; Gong, W.; Zhao, K.; Wang, Z.; Luo, J.; Li, C.; Sun, Y.; Xue, P.; Wang, C.; et al. Fluorescent fiber-shaped aqueous zinc-ion batteries for bifunctional multicolor-emission/energy-storage textiles. *ACS Nano* **2023**, *17*, 18494–18506. [[CrossRef](#)] [[PubMed](#)]
126. Shi, X.; Zuo, Y.; Zhai, P.; Shen, J.; Yang, Y.; Gao, Z.; Liao, M.; Wu, J.; Wang, J.; Xu, X.; et al. Large-area display textiles integrated with functional systems. *Nature* **2021**, *591*, 240–245. [[CrossRef](#)] [[PubMed](#)]
127. Chen, J.; Huang, Y.; Zhang, N.; Zou, H.; Liu, R.; Tao, C.; Fan, X.; Wang, Z. Micro-cable structured textile for simultaneously harvesting solar and mechanical energy. *Nat. Energy* **2016**, *1*, 16138. [[CrossRef](#)]
128. Chen, M.; Pang, D.; Chen, X.; Yan, H.; Yang, Y. Passive daytime radiative cooling: Fundamentals, material designs, and applications. *EcoMat* **2022**, *4*, e12153. [[CrossRef](#)]
129. Zheng, S.; Li, W.; Ren, Y.; Liu, Z.; Zou, X.; Hu, Y.; Guo, J.; Sun, Z.; Yan, F. Moisture-wicking, breathable, and intrinsically antibacterial electronic skin based on dual-gradient poly(ionic liquid) nanofiber membranes. *Adv. Mater.* **2022**, *34*, 2106570. [[CrossRef](#)] [[PubMed](#)]
130. Mo, F.; Liang, G.; Meng, Q.; Liu, Z.; Li, H.; Fan, J.; Zhi, C. A flexible rechargeable aqueous zinc manganese-dioxide battery working at 20 °C. *Energy Environ. Sci.* **2019**, *12*, 706–715. [[CrossRef](#)]
131. He, H.; Liu, J.; Wang, Y.; Zhao, Y.; Qin, Y.; Zhu, Z.; Yu, Z.; Wang, J. An ultralight self-powered fire alarm e-textile based on conductive aerogel fiber with repeatable temperature monitoring performance used in firefighting clothing. *ACS Nano* **2022**, *16*, 2953–2967. [[CrossRef](#)] [[PubMed](#)]
132. Chen, Z.; Wang, P.; Ji, Z.; Wang, H.; Liu, J.; Wang, J.; Hu, M.; Huang, Y. High-voltage flexible aqueous Zn-ion battery with extremely low dropout voltage and super-flat platform. *Nano-Micro Lett.* **2020**, *12*, 75. [[CrossRef](#)] [[PubMed](#)]
133. Fan, J.; Bao, B.; Wang, Z.; Li, H.; Wang, Y.; Chen, Y.; Wang, W.; Yu, D. Flexible, switchable and wearable image storage device based on light responsive textiles. *Chem. Eng. J.* **2021**, *404*, 126488. [[CrossRef](#)]
134. Park, J.; Choi, J.H.; Kong, K.; Han, J.; Park, J.; Kim, N.; Lee, E.; Kim, D.; Kim, J.; Chung, D.; et al. Electrically driven mid-submicrometre pixelation of InGaN micro-light-emitting diode displays for augmented-reality glasses. *Nat. Photonics* **2021**, *15*, 449–455. [[CrossRef](#)]
135. Park, J.; Kim, J.; Kim, S.-Y.; Cheong, W.H.; Jang, J.; Park, Y.-G.; Na, K.; Kim, Y.-T.; Heo, J.H.; Lee, C.Y.; et al. Soft, smart contact lenses with integrations of wireless circuits, glucose sensors, and displays. *Sci. Adv.* **2018**, *4*, eaap9841. [[CrossRef](#)] [[PubMed](#)]
136. Wang, Y.; Shen, R.; Wang, S.; Zhang, Y.-M.; Zhang, S.X.-A. Dynamic metal-ligand interaction of synergistic polymers for bistable see-through electrochromic devices. *Adv. Mater.* **2022**, *34*, 2104413. [[CrossRef](#)] [[PubMed](#)]
137. Ke, Y.; Chen, J.; Lin, G.; Wang, S.; Zhou, Y.; Yin, J.; Lee, P.S.; Long, Y. Smart windows: Electro-, thermo-, mechano-, photochromics, and beyond. *Adv. Energy Mater.* **2019**, *9*, 1902066. [[CrossRef](#)]
138. Wu, W.; Fang, H.; Ma, H.; Wu, L.; Wang, Q.; Wang, H. Self-powered rewritable electrochromic display based on WO<sub>3-x</sub> film with mechanochemically synthesized MoO<sub>3-y</sub> nanosheets. *ACS Appl. Mater. Interfaces* **2021**, *13*, 20326–20335. [[CrossRef](#)] [[PubMed](#)]

139. Li, X.; Yun, T.Y.; Kim, K.-W.; Kim, S.H.; Moon, H.C. Voltage-tunable dual image of electrostatic force-assisted dispensing printed, tungsten trioxide-based electrochromic devices with a symmetric configuration. *ACS Appl. Mater. Interfaces* **2020**, *12*, 4022–4030. [[CrossRef](#)] [[PubMed](#)]
140. Zhang, S.; Cao, S.; Zhang, T.; Yao, Q.; Fisher, A.; Lee, J. Monoclinic oxygen-deficient tungsten oxide nanowires for dynamic and independent control of near-infrared and visible light transmittance. *Mater. Horiz.* **2018**, *5*, 291–297. [[CrossRef](#)]
141. Alesanco, Y.; Viñuales, A.; Palenzuela, J.; Odriozola, I.; Cabañero, G.; Rodriguez, J.; Tena-Zaera, R. Multicolor electrochromics: Rainbow-like devices. *ACS Appl. Mater. Interfaces* **2016**, *8*, 14795–14801. [[CrossRef](#)] [[PubMed](#)]
142. Kanwat, A.; Ghosh, B.; Ng, S.; Rana, P.; Lekina, Y.; Hooper, T.; Yantara, N.; Kovalev, M.; Chaudhary, B.; Kajal, P.; et al. Reversible photochromism in <110> oriented layered halide perovskite. *ACS Nano* **2022**, *16*, 2942–2952. [[CrossRef](#)] [[PubMed](#)]
143. Du, Y.; Liu, S.; Li, Y.; Chen, X.; Ho, T.; Chao, L.; Tso, C. Perovskite-coated thermochromic transparent wood: A novel material for smart windows in energy-efficient and sustainable buildings. *ACS Appl. Mater. Interfaces* **2023**, *15*, 49665–49677. [[CrossRef](#)] [[PubMed](#)]
144. Ge, D.; Lee, E.; Yang, L.; Cho, Y.; Li, M.; Gianola, D.; Yang, S. A robust smart window: Reversibly switching from high transparency to angle-independent structural color display. *Adv. Mater.* **2015**, *27*, 2489–2495. [[CrossRef](#)] [[PubMed](#)]
145. Peng, J.; Cheng, Y.; Tomsia, A.; Jiang, L.; Cheng, Q. Thermochromic artificial nacre based on montmorillonite. *ACS Appl. Mater. Interfaces* **2017**, *9*, 24993–24998. [[CrossRef](#)] [[PubMed](#)]
146. Wang, Z.; Shi, X.; Peng, H. Alternating current electro-luminescent fibers for textile displays. *Natl. Sci. Rev.* **2023**, *10*, nwac113. [[CrossRef](#)] [[PubMed](#)]
147. Kim, W.; Kwon, S.; Lee, S.-M.; Kim, J.Y.; Han, Y.; Kim, E.; Choi, K.C.; Park, S.; Park, B.-C. Soft fabric-based flexible organic light-emitting diodes. *Org. Electron.* **2013**, *14*, 3007–3013. [[CrossRef](#)]
148. O'Connor, B.; An, K.H.; Zhao, Y.; Pipe, K.P.; Shtein, M. Fiber shaped light emitting device. *Adv. Mater.* **2007**, *19*, 3897–3900. [[CrossRef](#)]
149. Meier, S.B.; Tordera, D.; Pertegás, A.; Roldán-Carmona, C.; Ortí, E.; Bolink, H.J. Light-Emitting Electrochemical Cells: Recent Progress and Future Prospects. *Mater. Today* **2014**, *17*, 217–223. [[CrossRef](#)]
150. Zhang, Z.; Guo, K.; Li, Y.; Li, X.; Guan, G.; Li, H.; Luo, Y.; Zhao, F.; Zhang, Q.; Wei, B.; et al. A colour-tunable, weavable fibre-shaped polymer light-emitting electrochemical cell. *Nat. Photonics* **2015**, *9*, 233–238. [[CrossRef](#)]
151. Torres Alonso, E.; Rodrigues, D.P.; Khetani, M.; Shin, D.-W.; De Sanctis, A.; Joulie, H.; de Schrijver, I.; Baldycheva, A.; Alves, H.; Neves, A.I.S.; et al. Graphene electronic fibres with touch-sensing and light-emitting functionalities for smart textiles. *NPJ Flex. Electron.* **2018**, *2*, 25. [[CrossRef](#)]
152. Li, J.; Bisoyi, H.K.; Tian, J.; Guo, J.; Li, Q. Optically rewritable transparent liquid crystal displays enabled by light-driven chiral fluorescent molecular switches. *Adv. Mater.* **2019**, *31*, 1807751. [[CrossRef](#)] [[PubMed](#)]
153. Stranks, S.; Snaith, H. Metal-halide perovskites for photovoltaic and light-emitting devices. *Nat. Nanotechnol.* **2015**, *10*, 391–402. [[CrossRef](#)] [[PubMed](#)]
154. Ai, X.; Evans, E.W.; Dong, S.; Gillett, A.J.; Guo, H.; Chen, Y.; Hele, T.J.H.; Friend, R.H.; Li, F. Efficient radical-based light-emitting diodes with doublet emission. *Nature* **2018**, *563*, 536–540. [[CrossRef](#)] [[PubMed](#)]
155. Invernale, M.; Ding, Y.; Sotzing, G. All-organic electrochromic spandex. *ACS Appl. Mater. Interfaces* **2010**, *2*, 296–300. [[CrossRef](#)]
156. He, Z.; Wang, W.; Fan, J.; Bao, B.; Qin, X.; Yu, D. Photochromic microcapsules anchored on cotton fabric by layer-by-layer self-assembly method with erasable property. *React. Funct. Polym.* **2020**, *157*, 104762. [[CrossRef](#)]
157. Wang, Y.; Ren, J.; Ye, C.; Pei, Y.; Ling, S. Thermochromic silks for temperature management and dynamic textile displays. *Nano-Micro Lett.* **2021**, *13*, 72. [[CrossRef](#)] [[PubMed](#)]
158. Yang, W.; Lin, S.; Gong, W.; Lin, R.; Jiang, C.; Yang, X.; Hu, Y.; Wang, J.; Xiao, X.; Li, K.; et al. Single body-coupled fiber enables chipless textile electronics. *Science* **2024**, *384*, 74–81. [[CrossRef](#)] [[PubMed](#)]

**Disclaimer/Publisher's Note:** The statements, opinions and data contained in all publications are solely those of the individual author(s) and contributor(s) and not of MDPI and/or the editor(s). MDPI and/or the editor(s) disclaim responsibility for any injury to people or property resulting from any ideas, methods, instructions or products referred to in the content.